LETTER

doi:10.1038/nature14443

# The *Xist* lncRNA interacts directly with SHARP to silence transcription through HDAC3

Colleen A. McHugh[1]*, Chun-Kan Chen[1]*, Amy Chow[1], Christine F. Surka[1], Christina Tran[1], Patrick McDonel[2], Amy Pandya-Jones[3,4], Mario Blanco[1], Christina Burghard[1], Annie Moradian[5], Michael J. Sweredoski[5], Alexander A. Shishkin[1], Julia Su[1], Eric S. Lander[2], Sonja Hess[5], Kathrin Plath[3,4] & Mitchell Guttman[1]

**Many long non-coding RNAs (lncRNAs) affect gene expression[1], but the mechanisms by which they act are still largely unknown[2]. One of the best-studied lncRNAs is *Xist*, which is required for transcriptional silencing of one X chromosome during development in female mammals[3,4]. Despite extensive efforts to define the mechanism of *Xist*-mediated transcriptional silencing, we still do not know any proteins required for this role[3]. The main challenge is that there are currently no methods to comprehensively define the proteins that directly interact with a lncRNA in the cell[5]. Here we develop a method to purify a lncRNA from cells and identify proteins interacting with it directly using quantitative mass spectrometry. We identify ten proteins that specifically associate with *Xist*, three of these proteins—SHARP, SAF-A and LBR—are required for *Xist*-mediated transcriptional silencing. We show that SHARP, which interacts with the SMRT co-repressor[6] that activates HDAC3[7], is not only essential for silencing, but is also required for the exclusion of RNA polymerase II (Pol II) from the inactive X. Both SMRT and HDAC3 are also required for silencing and Pol II exclusion. In addition to silencing transcription, SHARP and HDAC3 are required for *Xist*-mediated recruitment of the polycomb repressive complex 2 (PRC2) across the X chromosome. Our results suggest that *Xist* silences transcription by directly interacting with SHARP, recruiting SMRT, activating HDAC3, and deacetylating histones to exclude Pol II across the X chromosome.**

Over the last two decades, numerous attempts have been made to define the protein complexes that interact with *Xist* and that are required for its various roles in X-chromosome inactivation (XCI)[3]. Most studies have used prior knowledge of the molecular events that occur on the X chromosome to define potential *Xist*-interacting proteins[8,9]. Although individual proteins that associate with *Xist* have been identified[8,10], we still do not know any of the proteins required for *Xist*-mediated transcriptional silencing because perturbations of these proteins, including components of the PRC2 complex, have no effect on *Xist*-mediated transcriptional silencing[11,12]. Current methods for identifying lncRNA-interacting proteins either require selection of specific candidate interacting proteins or fail to distinguish between direct RNA interactions that occur in the cell from those that merely associate in solution (reviewed in ref. 5).

To develop a method for identifying the proteins that directly interact with a specific lncRNA *in vivo*, we adapted our RNA antisense purification (RAP) method[13] to purify a lncRNA complex and identify the interacting proteins by quantitative mass spectrometry (RAP-MS) (Methods, Fig. 1a). Briefly, RAP-MS uses ultraviolet (UV) crosslinking to create covalent bonds between directly interacting RNA and protein and purifies lncRNAs in denaturing conditions to disrupt non-covalent interactions (Methods). This UV-crosslinking and denaturing approach, which is used by methods such as crosslinking and immunoprecipitation (CLIP), is known to identify only direct RNA–protein interactions and to separate interactions that are crosslinked in the cell from those that merely associate in solution[5,14].

Adapting this UV-crosslinking and denaturing approach to enable purification of a specific lncRNA is challenging for several reasons. (1) To purify lncRNA complexes in denaturing conditions, we need an RNA capture method that can withstand harsh denaturing conditions. (2) To detect the proteins associated with a given lncRNA, we need to achieve high purification yields of a lncRNA complex because, unlike nucleic acids, we cannot amplify proteins before detection. (3) Because any individual RNA is likely to be present at a very low percentage of the total cellular RNA, we need to achieve high levels of enrichment to identify specific interacting proteins. (4) Because the number of background proteins will be high, even after enrichment, we need accurate and sensitive methods for protein quantification to detect specific lncRNA-interacting proteins.

The RAP-MS method addresses these challenges because (1) RAP uses long biotinylated antisense probes, which form very stable RNA–DNA hybrids, and therefore can be used to purify lncRNA complexes in denaturing and reducing conditions (that is, 4 M urea at 67 °C, see Methods). (2) We optimized the RAP method to achieve high yields of endogenous RNA complexes. In our original protocol[13], we achieved <2% yield of the endogenous RNA complex; by optimizing hybridization, washing, and elution conditions (Methods), we were able to reproducibly achieve ~70% yield (Extended Data Fig. 1a, Methods). (3) Using our optimized conditions, we increased the enrichment levels for the target lncRNA complex (~5,000-fold, Extended Data Fig. 1b) relative to our already high levels of enrichment achieved previously (~100-fold)[13]. (4) To achieve sensitive quantification and to distinguish between specific proteins and background proteins, we used stable isotope labelling by amino acids in culture (SILAC) to label proteins (Methods, Extended Data Fig. 1c), which enables quantitative comparisons of purified proteins by mass spectrometry[15].

We validated the RAP-MS approach by defining the proteins that interact with two well-characterized non-coding RNAs: *U1* (a core component of the spliceosome) and *18S* (a component of the small ribosomal subunit). In the *U1* purifications, we identified 9 enriched proteins, all of which are known to interact with *U1* (Supplementary Note 1). In the *18S* purification, we identified 105 enriched proteins; 98 of these (93%) were previously characterized as ribosomal proteins, ribosomal processing and assembly factors, translational regulators, or other known ribosome interactors (Extended Data Fig. 2). In particular, we identified 21 of the 31 known small ribosomal subunit proteins. The few missing proteins appear to fall predominately into two categories: proteins that make few direct contacts with the RNA and small proteins that contain few peptides that could be detected by mass spectrometry.

[1]Division of Biology and Biological Engineering, California Institute of Technology, Pasadena, California 91125, USA. [2]Broad Institute of MIT and Harvard, Cambridge, Massachusetts 02139, USA. [3]Department of Biological Chemistry, Jonsson Comprehensive Cancer Center, Molecular Biology Institute, University of California Los Angeles, Los Angeles, California 90095, USA. [4]Eli and Edythe Broad Center of Regenerative Medicine and Stem Cell Research, David Geffen School of Medicine, University of California Los Angeles, Los Angeles, California 90095, USA. [5]Proteome Exploration Laboratory, Beckman Institute, California Institute of Technology, Pasadena, California 91125, USA.
*These authors contributed equally to this work.

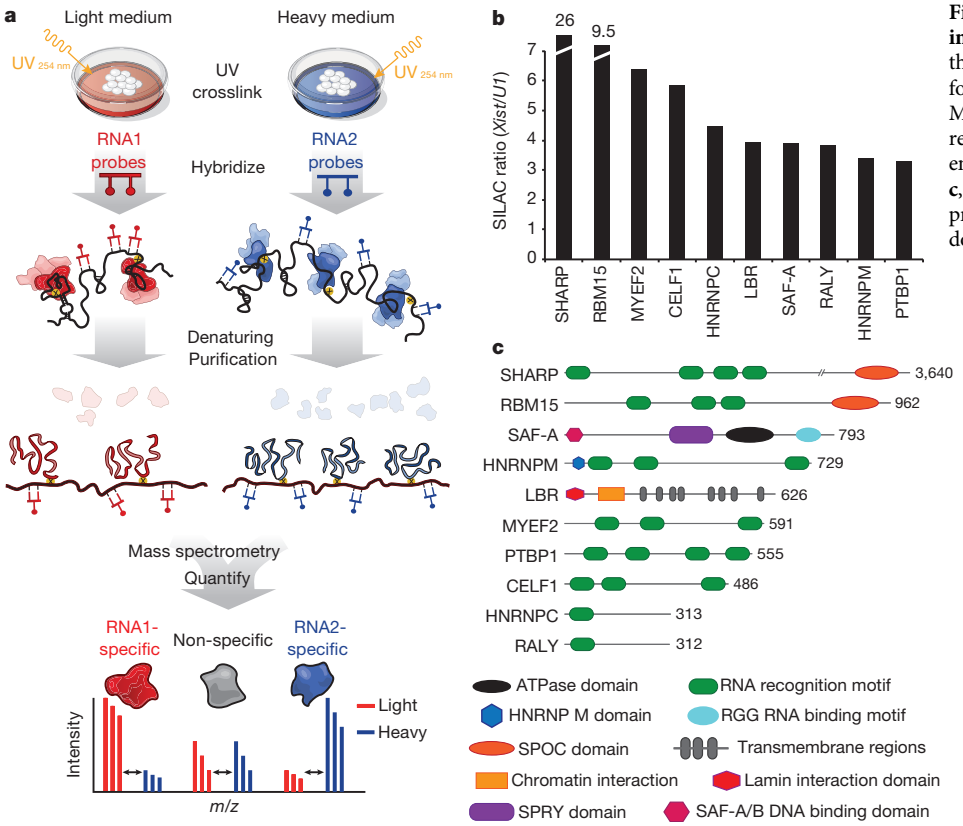


**Figure 1 | RAP-MS identifies direct *Xist*-interacting proteins.** **a**, A schematic overview of the RAP-MS method. **b**, The SILAC ratio (*Xist*/U1) for each *Xist*-enriched protein identified by RAP-MS for one representative sample of four biological replicates. For SHARP and RBM15, the enrichment values are indicated above their bars. **c**, Each *Xist*-interacting protein is shown (scaled to protein length). The locations of functional domains are shown.

These results demonstrate that the RAP-MS method identifies the majority of known RNA-interacting proteins, and that the proteins identified by RAP-MS are highly specific for the purified ncRNA complex.

To define the proteins that interact with *Xist* during the initiation of XCI, we UV-crosslinked SILAC-labelled mouse embryonic stem (ES) cells after *Xist* induction[13] and purified *Xist* from nuclear extracts (Methods). To control for background proteins or non-specific proteins that might interact with any nuclear RNA, we separately purified the abundant U1 small nuclear RNA, which is not expected to interact with the same proteins as *Xist*. We identified the proteins in each sample using liquid chromatography-mass spectrometry and calculated a SILAC ratio for each protein based on the intensity of all heavy or light peptides originating from the *Xist* or *U1* purification (Fig. 1a, Methods).

We identified 10 proteins that were enriched for *Xist* relative to *U1* (SILAC ratio >threefold, Fig. 1b). All 10 proteins were reproducibly enriched in multiple *Xist* purifications from independent biological samples (Methods). Consistent with the notion that these proteins are direct *Xist*-interacting proteins, 9 proteins contain well-characterized RNA binding domains (Fig. 1c).

The identified *Xist*-interacting proteins are SHARP, RBM15, MYEF2, CELF1, HNRNPC, LBR, SAF-A, RALY, HNRNPM, and PTBP1 (Fig. 1b). SAF-A (scaffold attachment factor-A, also known as HNRNPU) was previously shown to interact directly with *Xist* and is required for tethering *Xist* to the inactive X chromosome in differentiated cells[10]. In addition, 5 of these proteins have been previously implicated in transcriptional repression, chromatin regulation, and nuclear organization. These include SHARP (SMRT and HDAC associated repressor protein, also known as SPEN), a member of the SPEN family of transcriptional repressors, which directly interacts with the SMRT component (also known as NCOR2) of the nuclear co-repressor complex[16] that is known to interact with and activate HDAC3 deacetylation activity on chromatin[7] (Fig. 1c). Interestingly, we also identified RBM15, another member of the SPEN family of transcriptional repressors, which shares the same domain structure as SHARP, but seems to have a distinct functional role during development[17]. MYEF2 has been shown to function as a negative regulator of transcription in multiple cell types, although its mechanism of regulation is still unknown[18]. HNRNPM is a paralogue of MYEF2. Finally, we identified LBR (lamin B receptor), a protein that is anchored in the inner nuclear membrane and interacts with repressive chromatin regulatory proteins and lamin B[19] (Fig. 1c).

We confirmed the specificity of the identified *Xist*-interacting proteins (Supplementary Note 2, Methods). To ensure that they were not identified owing to non-specific RNA or protein capture, we performed RAP in uninduced cells (no *Xist*) and identified no enriched proteins. To ensure that these proteins are crosslinked with *Xist* in cells and not merely associating in solution, we performed RAP in cells that were not crosslinked (no UV) and identified no enriched proteins. To ensure that these proteins do not merely interact with any nuclear-enriched long ncRNA, we compared the *Xist*-purified proteins to those purified with 45S (pre-ribosomal RNA) and found that all 10 *Xist*-interacting proteins were still enriched. Finally to validate these interactions independently, we obtained high-quality affinity reagents for 8 of the 10 proteins (PTBP1, HNRNPC, CELF1, MYEF2, RBM15, LBR, RALY and SHARP), and immunoprecipitated the identified proteins in UV-crosslinked lysates. In all cases, we observed a strong enrichment for the *Xist* RNA (>fourfold), but not control mRNAs or lncRNAs (Extended Data Fig. 3, Supplementary Table 1).

Together, these results identify a set of highly specific and reproducible proteins that interact directly with *Xist* during the initiation of XCI. Given the generality of the RAP-MS approach, we expect that it will be broadly applicable for defining the proteins that interact directly with other lncRNAs.

To determine which proteins are required for *Xist*-mediated transcriptional silencing, we knocked down each of the proteins identified and assayed for the failure to silence gene expression on the X chromosome upon induction of *Xist* expression (Fig. 2a).

Specifically, we selected two X-linked genes, *Gpc4* and *Atrx*, that are well expressed in the absence of *Xist* expression, but are normally silenced by 16 h of *Xist* induction in our doxycycline-inducible system

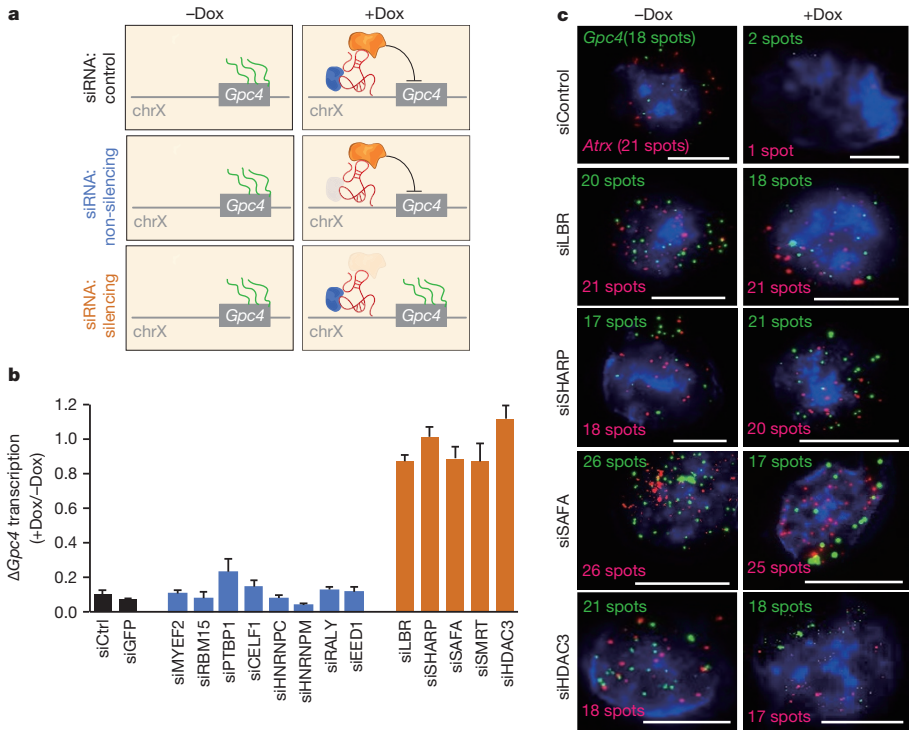


**Figure 2 | SHARP, LBR and SAF-A are required for *Xist*-mediated gene silencing.** **a**, Screen for *Xist*-mediated gene silencing for knockdown of control (top), non-silencing proteins (middle), or silencing proteins (bottom). **b**, *Gpc4* mRNA levels after induction of *Xist* (+Dox) normalized to *Gpc4* levels before *Xist* induction (−Dox). Error bars, standard error of the mean across 50 cells from one experiment. siCtrl, scrambled siRNA control. **c**, Images of individual cells for two X-linked mRNAs, *Gpc4* (green) and *Atrx* (red), and DAPI (blue) after treatment with different siRNAs (rows). The number of identified mRNAs is shown. Scale bars, 5 μm.

in male cells (Fig. 2b, Methods). We used short interfering RNAs (siRNAs) to knockdown the messenger RNA levels of each of the proteins identified by RAP-MS along with several negative controls (Methods, Supplementary Table 2). We ensured that each cell examined showed both successful depletion of the siRNA-targeted mRNA (>70% reduction) as well as induction of *Xist* expression using single-molecule RNA fluorescence *in situ* hybridization (FISH; Methods). Within each of these cells, we quantified the mRNA level of each of the two X-linked genes before *Xist* induction (−Dox) and after *Xist* induction (+Dox).

As a control, we transfected several non-targeting siRNAs (Methods). In these negative controls, we observed the expected silencing of the X-linked genes studied (*Gpc4* transcript levels decreased from an average of 20 copies (−Dox) to 2 copies (+Dox) per cell and *Atrx* transcript levels decreased from 22 to 3 copies per cell; Fig. 2b, c). Consistent with previous observations, we found no effect on X chromosome gene silencing upon knockdown of EED[20,21], a required component of PRC2[22] (Fig. 2b), or other proteins previously associated with *Xist* that do not seem to be required for transcriptional silencing (Extended Data Fig. 4, Methods). Similarly, knockdown of RBM15, MYEF2, PTBP1, CELF1, HNRNPC, RALY or HNRNPM did not alter gene silencing on the X chromosome (Fig. 2b, Extended Data Fig. 5).

In contrast, knockdown of SHARP, LBR or SAF-A largely abolished the silencing of X chromosome genes following *Xist* induction (Fig. 2b, c, Supplementary Note 3, Extended Data Figs 5, 6). Indeed, the expression levels of the X chromosome genes studied did not significantly change following *Xist* expression (Fig. 2c, Extended Data Fig. 5). These same silencing defects were observed with several independent siRNAs (Extended Data Fig. 7). Importantly, we observed the same X chromosome silencing defects upon knockdown of SHARP, LBR or SAF-A in differentiating female ES cells (Extended Data Fig. 8, Methods).

These results demonstrate that SHARP, LBR and SAF-A are required for *Xist*-mediated transcriptional silencing of the X chromosome. Although the remaining seven *Xist*-interacting proteins showed no effect on X-chromosome gene silencing, they may still be important for *Xist* function. Some may have redundant functions (for example, MYEF2 and HNRNPM, which are known paralogues), in some of these cases, the small amount of protein remaining after knockdown may still be sufficient for *Xist* function, or some of these proteins may be important for alternative *Xist*-mediated roles, such as the maintenance of XCI, which would not be captured by this silencing assay.

*Xist* initiates XCI by spreading across the future inactive X chromosome, excluding RNA polymerase II (Pol II), and repositioning active genes into a transcriptionally silenced nuclear compartment[3,10,13,23]. All of these roles—localization, RNA Pol II exclusion and repositioning—are required for proper silencing of transcription during the initiation of XCI[3].

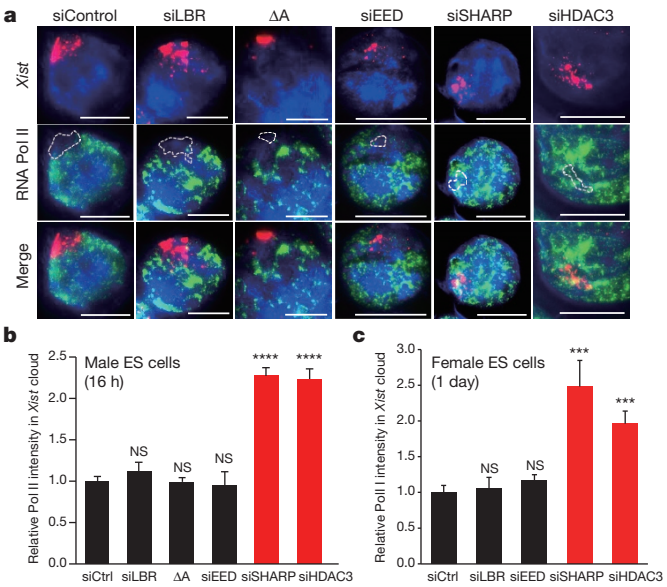


**Figure 3 | SHARP is required for exclusion of Pol II from the *Xist*-coated territory.** **a**, *Xist* (red), Pol II (green) and DAPI (blue) across different siRNA conditions (rows). **b**, **c**, Quantification of fluorescence intensity of Pol II within *Xist* territory normalized to control siRNA levels for male ES cells after 16 h of doxycycline treatment (**b**) and female ES cells after 1 day of retinoic-acid-induced differentiation (**c**). Error bars, standard error of the mean across 50 cells from one experiment. NS, not significant; ***$P$ value < 0.005, ****$P$ value < 0.001 relative to siControl by unpaired two-sample $t$-test. ΔA, genetic deletion of A-repeat of *Xist*. Scale bars, 5 μm.

Consistent with previous observations that SAF-A is required for *Xist* localization to chromatin in differentiated cells[10], we observed a diffuse *Xist* localization pattern in the nucleus upon knockdown of SAF-A (Extended Data Fig. 5). This suggests that SAF-A is required for transcriptional silencing by localizing *Xist*, and its silencing proteins, to the X chromosome during the initiation of XCI.

To determine the proteins responsible for establishing the initial silenced compartment on the X chromosome, we explored whether SHARP or LBR are required for the exclusion of Pol II from the *Xist*-coated region. Specifically, we measured the co-localization of *Xist* and Pol II in single cells (Methods). In wild-type cells after 16 h of *Xist* induction, we observed a depletion of Pol II over the *Xist*-coated territory (Fig. 3a, Methods). We observed a similar exclusion of Pol II from the *Xist*-coated region in the negative controls and upon knockdown of EED or LBR (Fig. 3a, b). In contrast, upon knockdown of SHARP, we observed higher levels of Pol II over the *Xist*-coated territory relative to the control samples (Fig. 3b). We confirmed that SHARP, but not LBR or EED, is similarly required for Pol II exclusion in differentiating female ES cells (Fig. 3c, Extended Data Fig. 9, Supplementary Note 4).

These results demonstrate that SHARP is required to exclude Pol II on the inactive X chromosome and may be required for creating the initial silenced compartment upon *Xist* localization[3]. Although LBR is not required for Pol II exclusion, it is likely to have an alternative role during the initiation of *Xist*-mediated transcriptional silencing, such as repositioning genes into this Pol II-excluded compartment[13,23].

Having identified SHARP as the direct *Xist*-interacting protein that is required for excluding Pol II on the X chromosome, we sought to determine how it might carry out this role. SHARP is a direct RNA binding protein[6,24] that was first identified in mammals on the basis of its interaction with the SMRT co-repressor complex[6], which is known to interact with HDAC3 and is required for activating its deacetylation and transcriptional silencing activity *in vivo*[7]. Based on these previous observations, we hypothesized that *Xist*-mediated transcriptional silencing through SHARP would occur through SMRT and the silencing function of HDAC3. (We would not expect to identify these proteins by RAP-MS, which was designed to identify only direct RNA–protein interactions.)

To test this hypothesis, we knocked down either SMRT or HDAC3 and measured the expression of X chromosome genes upon *Xist* induction. Knockdown of SMRT or HDAC3 in both male and female ES cells abrogated silencing of X chromosome genes upon induction of *Xist* expression (Fig. 2b, Extended Data Figs 5, 7 and 8). To ensure that the observed silencing defect is specific for HDAC3 and not for other class I HDAC proteins, we knocked down HDAC1 or HDAC2 and observed no effect on gene silencing (Extended Data Fig. 5). To further confirm the specificity of our results, we used independent siRNAs to knockdown SMRT or HDAC3 and in all cases identified a similar silencing defect (Extended Data Fig. 7).

To determine whether this effect is similar to the effect produced by knockdown of SHARP or a distinct defect in transcriptional silencing, we tested whether HDAC3, the silencing protein in this complex[7,25], is required for the exclusion of RNA Pol II from the *Xist*-coated territory. We found that knockdown of HDAC3 in both male and female ES cells eliminated the exclusion of RNA Pol II from the *Xist*-coated compartment to a similar degree to that seen for knockdown of SHARP (Fig. 3, Extended Data Fig. 9).

These results suggest that SHARP silences transcription through SMRT and the HDAC3 silencing protein. This role for HDAC3 in *Xist*-mediated silencing would explain the long-standing observation of global hypoacetylation on the entire X chromosome as one of the very first events that occur upon initiation of XCI[3,26].

One of the features of XCI is the recruitment of PRC2 and its associated H3K27me3 repressive chromatin modifications across the X chromosome in an *Xist*-dependent manner[3,4,9]. Although PRC2 is not required for the initiation of XCI[11,12] (Fig. 3b), it or its associated

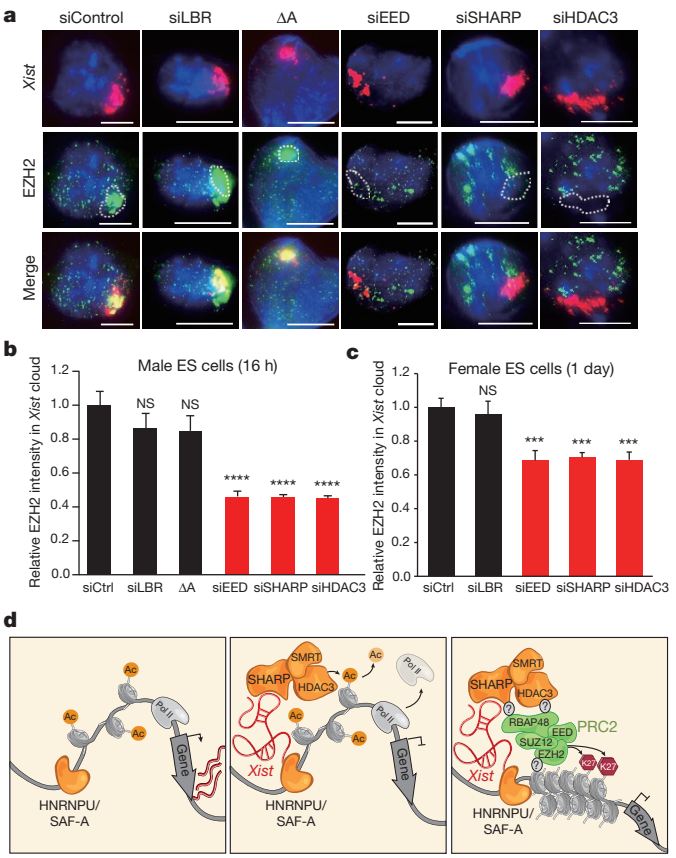


**Figure 4 | SHARP is required for PRC2 recruitment across the *Xist*-coated territory.** **a**, *Xist* (red), EZH2 (green) and DAPI (blue) across siRNA conditions (rows). **b**, **c**, Quantification of EZH2 levels within the defined *Xist* territory normalized to the levels in the control siRNA sample for male ES cells (**b**) and differentiating female ES cells (**c**). Error bars, standard error of the mean across 50 cells from one experiment. NS, not significant; ***$P$ value $< 0.005$, ****$P$ value $< 0.001$ relative to siControl by an unpaired two-sample $t$-test. Scale bars, 5 μm. **d**, A model for *Xist*-mediated transcriptional silencing and recruitment of PRC2 across the X chromosome.

H3K27me3 repressive chromatin modifications may be involved in establishing an epigenetically silenced state[27]. Yet, how *Xist* recruits the PRC2 complex across the X chromosome is unknown. Since we failed to identify any PRC2 components by RAP-MS, and various HDAC complexes are known to recruit PRC2[28], we hypothesized that PRC2-recruitment is mediated by SHARP and HDAC3.

To test this hypothesis, we looked at PRC2 recruitment to the *Xist*-coated territory. In wild-type cells, we observe a strong enrichment of EZH2, a component of PRC2, over the *Xist*-coated territory after 16 h of induction (Fig. 4a). Upon knockdown of EED, a distinct component of the PRC2 complex that is required for its proper localization to chromatin[22], we observe no enrichment of EZH2 over the *Xist*-coated territory at this same time point (Fig. 4a). Similarly, upon knockdown of SHARP, we identified a loss of EZH2 over the *Xist*-coated territory, of comparable magnitude to that observed in the absence of EED (Fig. 4a). Conversely, upon knockdown of LBR, we observed a strong enrichment of EZH2 over the *Xist*-coated territory, of comparable magnitude to the levels of recruitment in wild-type conditions (Fig. 4b). To determine whether HDAC3 is required for PRC2 recruitment, we knocked down HDAC3 and observed a loss of PRC2 recruitment (Fig. 4a), of comparable magnitude to that observed upon loss of SHARP (Fig. 4b). Knockdown of SHARP or HDAC3 led to the same PRC2-recruitment defect in female ES cells (Fig. 4c, Extended Data Fig. 10).

These results indicate that *Xist*-mediated recruitment of PRC2 across the X chromosome is dependent on SHARP and HDAC3. Whether this occurs through an interaction with SHARP or HDAC3

(direct recruitment) or due to the HDAC3-induced silenced transcription state, chromatin modifications, or compact chromatin structure (indirect recruitment) remains unclear (Supplementary Note 5). Yet, our results are in contrast to a previous model that PRC2 is recruited through a direct interaction between EZH2 and the A-repeat of *Xist*[8]. The evidence for this PRC2–*Xist* interaction is based on *in vitro* binding and purifications in non-denaturing conditions[8]. Recently, the specificity of this interaction has been questioned because PRC2 appears to bind promiscuously to many RNAs, including bacterial RNAs, in these conditions[29]. Instead, our results are consistent with reports that deletion of the A-repeat, unlike knockdown of SHARP or HDAC3, has no significant effect on PRC2 recruitment to the *Xist*-coated territory[9] (Fig. 4b).

Taken together, our data suggest a model for how *Xist* can orchestrate transcriptional silencing on the X chromosome (Fig. 4d). Upon initiation of *Xist* expression, *Xist* can localize to sites on the X chromosome by binding to the SAF-A protein[10], which is known to interact directly with chromatin[30]. *Xist* interacts directly with SHARP to recruit SMRT[6] to these DNA sites across the inactive X chromosome. This *Xist*–SHARP–SMRT complex either recruits HDAC3 directly to the X chromosome or may act to induce the enzymatic activity of HDAC3[7] that may already be present at active genes across the X chromosome[31]. Through HDAC3, *Xist* can direct the removal of activating histone acetylation marks on chromatin, thereby compacting chromatin and silencing transcription[32]. Upon initiating the silenced state, *Xist* recruits PRC2 across the X chromosome in an HDAC3-dependent manner, either through a direct interaction between PRC2 and HDAC3 or indirectly through HDAC3-induced transcriptional silencing or chromatin compaction (Supplementary Note 5). In this way, the same *Xist*-interacting protein might achieve two essential roles in XCI: initiating the inactive state by recruiting transcriptional silencers (HDAC3) and maintaining the inactive state by recruiting stable epigenetic silencers (PRC2)[27]. Beyond *Xist*, RAP-MS provides a critical tool that will accelerate the discovery of novel lncRNA mechanisms that have thus far proved elusive.

**Online Content** Methods, along with any additional Extended Data display items and Source Data, are available in the online version of the paper; references unique to these sections appear only in the online paper.

**Received 25 November 2014; accepted 2 April 2015.**
**Published online 27 April 2015.**

1. Guttman, M. *et al.* lincRNAs act in the circuitry controlling pluripotency and differentiation. *Nature* **477,** 295–300 (2011).
2. Rinn, J. L. & Chang, H. Y. Genome regulation by long noncoding RNAs. *Annu. Rev. Biochem.* **81,** 145–166 (2012).
3. Wutz, A. Gene silencing in X-chromosome inactivation: advances in understanding facultative heterochromatin formation. *Nature Rev. Genet.* **12,** 542–553 (2011).
4. Lee, J. T. Lessons from X-chromosome inactivation: long ncRNA as guides and tethers to the epigenome. *Genes Dev.* **23,** 1831–1842 (2009).
5. McHugh, C. A., Russell, P. & Guttman, M. Methods for comprehensive experimental identification of RNA-protein interactions. *Genome Biol.* **15,** 203 (2014).
6. Shi, Y. *et al.* Sharp, an inducible cofactor that integrates nuclear receptor repression and activation. *Genes Dev.* **15,** 1140–1151 (2001).
7. You, S. H. *et al.* Nuclear receptor co-repressors are required for the histone-deacetylase activity of HDAC3 *in vivo*. *Nature Struct. Mol. Biol.* **20,** 182–187 (2013).
8. Zhao, J., Sun, B. K., Erwin, J. A., Song, J. J. & Lee, J. T. Polycomb proteins targeted by a short repeat RNA to the mouse X chromosome. *Science* **322,** 750–756 (2008).
9. Plath, K. *et al.* Role of histone H3 lysine 27 methylation in X inactivation. *Science* **300,** 131–135 (2003).
10. Hasegawa, Y., Brockdorff, N., Kawano, S., Tsutui, K. & Nakagawa, S. The matrix protein hnRNP U is required for chromosomal localization of Xist RNA. *Dev. Cell* **19,** 469–476 (2010).
11. Schoeftner, S. *et al.* Recruitment of PRC1 function at the initiation of X inactivation independent of PRC2 and silencing. *EMBO J.* **25,** 3110–3122 (2006).
12. Kalantry, S. & Magnuson, T. The Polycomb group protein EED is dispensable for the initiation of random X-chromosome inactivation. *PLoS Genet.* **2,** e66 (2006).
13. Engreitz, J. M. *et al.* The Xist lncRNA exploits three-dimensional genome architecture to spread across the X chromosome. *Science* **341,** 1237973 (2013).
14. Darnell, R. B. HITS-CLIP: panoramic views of protein–RNA regulation in living cells. *Wiley Interdiscipl. Rev. RNA* **1,** 266–286 (2010).
15. Ong, S. E. & Mann, M. A practical recipe for stable isotope labeling by amino acids in cell culture (SILAC). *Nature Protoc.* **1,** 2650–2660 (2007).
16. Ariyoshi, M. & Schwabe, J. W. A conserved structural motif reveals the essential transcriptional repression function of Spen proteins and their role in developmental signaling. *Genes Dev.* **17,** 1909–1920 (2003).
17. Raffel, G. D. *et al.* Ott1(Rbm15) has pleiotropic roles in hematopoietic development. *Proc. Natl Acad. Sci. USA* **104,** 6001–6006 (2007).
18. Haas, S., Steplewski, A., Siracusa, L. D., Amini, S. & Khalili, K. Identification of a sequence-specific single-stranded DNA binding protein that suppresses transcription of the mouse myelin basic protein gene. *J. Biol. Chem.* **270,** 12503–12510 (1995).
19. Olins, A. L., Rhodes, G., Welch, D. B., Zwerger, M. & Olins, D. E. Lamin B receptor: multi-tasking at the nuclear envelope. *Nucleus* **1,** 53–70 (2010).
20. Brown, C. J. & Baldry, S. E. Evidence that heteronuclear proteins interact with XIST RNA *in vitro*. *Somat. Cell Mol. Genet.* **22,** 403–417 (1996).
21. Sarma, K. *et al.* ATRX directs binding of PRC2 to Xist RNA and Polycomb targets. *Cell* **159,** 869–883 (2014).
22. Margueron, R. & Reinberg, D. The Polycomb complex PRC2 and its mark in life. *Nature* **469,** 343–349 (2011).
23. Chaumeil, J., Le Baccon, P., Wutz, A. & Heard, E. A novel role for Xist RNA in the formation of a repressive nuclear compartment into which genes are recruited when silenced. *Genes Dev.* **20,** 2223–2237 (2006).
24. Arieti, F. *et al.* The crystal structure of the Split End protein SHARP adds a new layer of complexity to proteins containing RNA recognition motifs. *Nucleic Acids Res.* **42,** 6742–6752 (2014).
25. Li, J., Lin, Q., Wang, W., Wade, P. & Wong, J. Specific targeting and constitutive association of histone deacetylase complexes during transcriptional repression. *Genes Dev.* **16,** 687–692 (2002).
26. Keohane, A. M., O'Neill, L. P., Belyaev, N. D., Lavender, J. S. & Turner, B. M. X-inactivation and histone H4 acetylation in embryonic stem cells. *Dev. Biol.* **180,** 618–630 (1996).
27. Riising, E. M. *et al.* Gene silencing triggers polycomb repressive complex 2 recruitment to CpG islands genome wide. *Mol. Cell* **55,** 347–360 (2014).
28. van der Vlag, J. & Otte, A. P. Transcriptional repression mediated by the human polycomb-group protein EED involves histone deacetylation. *Nature Genet.* **23,** 474–478 (1999).
29. Davidovich, C., Zheng, L., Goodrich, K. J. & Cech, T. R. Promiscuous RNA binding by Polycomb repressive complex 2. *Nature Struct. Mol. Biol.* **20,** 1250–1257 (2013).
30. Fackelmayer, F. O., Dahm, K., Renz, A., Ramsperger, U. & Richter, A. Nucleic-acid-binding properties of hnRNP-U/SAF-A, a nuclear-matrix protein which binds DNA and RNA *in vivo* and *in vitro*. *Eur. J. Biochem.* **221,** 749–757 (1994).
31. Wang, Z. *et al.* Genome-wide mapping of HATs and HDACs reveals distinct functions in active and inactive genes. *Cell* **138,** 1019–1031 (2009).
32. Kuo, M. H. & Allis, C. D. Roles of histone acetyltransferases and deacetylases in gene regulation. *Bioessays* **20,** 615–626 (1998).

**Supplementary Information** is available in the online version of the paper.

**Acknowledgements** We thank J. Engreitz for extensive discussions, help in adapting the RAP method, and critical comments on the manuscript; A. Gnirke, S. Carr, J. Jaffe and M. Schenone for initial discussions about the RAP-MS method; A. Collazo, E. Lubek, and L. Cai for microscopy help; A. Wutz for providing transgenic cell lines; R. Eggleston-Rangel for assistance with mass spectrometry; S. Grossman, I. Amit, M. Garber and J. Rinn for comments on the manuscript and helpful suggestions; and S. Knemeyer for illustrations. C.A.M. is supported by a post-doctoral fellowship from Caltech. C.-K.C. is supported by an NIH NRSA training grant (T32GM07616). Imaging was performed in the Biological Imaging Facility, with the support of the Caltech Beckman Institute and the Arnold and Mabel Beckman Foundation. This work was funded by the Gordon and Betty Moore Foundation (GBMF775), the Beckman Institute, and NIH (1S10RR029591-01A1 to S.H.), an NIH Director's Early Independence Award (DP5OD012190), the Rose Hills Foundation, Edward Mallinckrodt Foundation, Sontag Foundation, Searle Scholars Program, and funds from the California Institute of Technology.

**Author Contributions** C.A.M. developed the RAP-MS method, designed, performed, and analysed RAP-MS experiments and data, C.-K.C. designed, performed, and analysed *Xist* functional experiments, A.C. designed, performed, and oversaw experiments, C.F.S. helped develop RAP-MS and performed experiments, C.T., P.M., A.P.-J., A.M., A.A.S., J.S. performed experiments, M.J.S., M.B., C.B. analysed data, E.S.L. helped develop initial ideas for adapting RAP for protein detection, S.H. oversaw mass spectrometry development and data analysis, K.P. helped design *Xist* RAP-MS and functional experiments and analysed data, M.G. conceived, designed and oversaw the entire project and integrated the data, C.A.M., C.-K.C. and M.G. wrote the manuscript with input from all authors.

**Author Information** Reprints and permissions information is available at www.nature.com/reprints. The authors declare no competing financial interests. Readers are welcome to comment on the online version of the paper. Correspondence and requests for materials should be addressed to M.G. (mguttman@caltech.edu).

## METHODS

No statistical methods were used to predetermine sample size. Detailed RAP-MS protocols are available at the authors' web site: (http://www.lncrna.caltech.edu/RAP).

**Mouse ES cell culture.** All mouse ES cell lines were cultured in serum-free 2i/LIF medium as previously described[13]. We used the following cell lines: wild-type male ES cells (V6.5 line); male ES cells expressing *Xist* from the endogenous locus under control of a tet-inducible promoter (pSM33 ES cell line) as previously described[13]; male ES cells carrying a cDNA *Xist* transgene without the A-repeat integrated into the *Hprt* locus under control of the tet-inducible promoter (A-repeat deletion: provided by A. Wutz)[33]; female ES cells (F1 2-1 line). This wild-type female mouse ES cell line is derived from a 129 × castaneous F1 mouse cross as previously described[13].

***Xist* induction.** For Dox inducible cells (pSM33 and A-repeat deletion), we induced *Xist* expression by treating cells with 2 μg ml$^{-1}$ doxycycline (Sigma) for 6 h, 16 h, or 24 h based on the application. For female ES cells (F1 2-1 line), we induced *Xist* expression by inducing differentiation; 2i was replaced with MEF media (DMEM, 10% Gemini Benchmark FBS, 1 × L-glutamine, 1 × NEAA, 1 × penicillin/streptomycin; Life Technologies unless otherwise indicated) for 24 h followed by treatment with 1 μM retinoic acid (RA) (Sigma) for an additional 24 h.

We measured the amount of *Xist* RNA in both the doxycycline-inducible cells (6 h induction) and differentiating female ES cells (24 h induction) by qRT–PCR. We normalized this level to various RNA housekeeping controls, 18S, 28S, and U6, in both cell populations and calculated the fold expression difference between male and female cells using the comparative Ct method. We observed a range of expression, with the male inducible system expressing from 5 to 20-fold (12-fold average) more *Xist* than the female cells. We note that this estimate likely represents an upper limit of the actual differences because the female ES cell system is known to be heterogeneous in *Xist*-induction, such that not every cell will induce *Xist* to the same level after 24 h of retinoic acid treatment. Accordingly, we expect that the actual differences between the male inducible system and differentiating female ES cells are actually significantly lower. While the precise levels are hard to compare by single molecule FISH, the size and intensity of each *Xist* RNA-coated territory is similar in both systems at the time points used.

The male-inducible system is more sensitive for identifying proteins that affect silencing compared to a female system because *Xist*-mediated silencing in males will lead to loss of 100% of X-chromosome transcripts rather than only 50% in a female system, which still retains one active X.

**UV crosslinking.** Cells were washed once with PBS and then crosslinked on ice using 0.8 J cm$^{-2}$ (UV8k) of UV at 254 nm in a Spectrolinker UV Crosslinker. Cells were then scraped from culture dishes, washed once with PBS, pelleted by centrifugation at 1,500*g* for 4 min, and flash-frozen in liquid nitrogen for storage at –80 °C.

**SILAC ES cell culture.** For SILAC experiments, we adapted our ES cell culture procedures to incorporate either light or heavy lysine and arginine amino acids. The 2i/LIF SILAC medium was composed as follows: custom DMEM/F-12 without lysine or arginine (Dundee Cell Products) was supplemented with either 0.398 mM heavy Arg10 (Sigma) or unlabelled arginine (Sigma) and either 0.798 mM heavy Lys8 (Cambridge Isotope Labs) or unlabelled lysine (Sigma), 0.5 × B-27 (Gibco), 2 mg ml$^{-1}$ bovine insulin (Sigma), 1.37 μg ml$^{-1}$ progesterone (Sigma), 5 mg ml$^{-1}$ BSA Fraction V (Gibco), 0.1 mM 2-mercaptoethanol (Sigma), 5 ng ml$^{-1}$ murine LIF (GlobalStem), 0.1 μM PD0325901 (SelleckChem) and 0.3 μM CHIR99021 (SelleckChem). Cells in both heavy and light 2i/LIF SILAC medium were also supplemented with 0.2 mg ml$^{-1}$ of unlabelled proline (Sigma) to prevent conversion of labelled arginine to proline. 2i inhibitors were added fresh with each medium change.

**Adapting cells to SILAC conditions.** Prior to mass spectrometry, ES cells were adapted to SILAC conditions over three passages. The heavy or light culture medium was replaced every 24–48 h depending on cell density, and cells were passaged every 72 h using 0.025% trypsin (Gibco), rinsing dissociated cells from the plates with DMEM/F12 containing 0.038% BSA Fraction V (Gibco). Cells were grown in two different types of medium: 2i/LIF SILAC medium with light (unlabelled) lysine and arginine, or 2i/LIF SILAC medium with heavy isotope-labelled lysine and arginine.

**Measuring SILAC incorporation.** To examine the efficiency of SILAC labelling in pSM33 cells, we tested for the incorporation of labelled amino acids after 10 days of growth (3 cell passages) in heavy 2i/LIF SILAC medium. Pellets of 2 million cells were boiled for 10 min in LDS Sample Loading Buffer (Invitrogen) and then proteins were separated by SDS–PAGE on a 4–12% Tris-Glycine polyacrylamide gel (Invitrogen). Total protein was stained with Colloidal Coomassie (Invitrogen) and gel slices were excised with a clean scalpel and transferred to microcentrifuge tubes for in-gel tryptic digest. Protein disulphide bonds were reduced with DTT then alkylated with iodoacetamide. Proteins were digested with trypsin overnight and then extracted using successive washes with 1% formic acid/2% acetonitrile, 1:1 acetonitrile/water, and 1% formic acid in acetonitrile. Peptides were collected, lyophilized, then resuspended in 1% formic acid for mass spectrometry analysis (described later in Mass spectrum measurements). Peptides were identified from mass spectra using MaxQuant (described later in Mass spectrometry data analysis). The incorporation rate of labelled amino acids was calculated based on the ratio of the intensity of heavy and light versions of each peptide identified. In cells used for subsequent assays, we confirmed that over 95% of peptides from cellular proteins showed >95% incorporation of labelled amino acids (Extended Data Fig. 1b).

**RNA antisense purification-mass spectrometry (RAP-MS).** *Probe design and generation.* To create the probes used to capture target RNAs, we designed and synthesized 90-mer DNA oligonucleotides (Eurofins Operon) that spanned the entire length of the target RNA. The sequence of each DNA oligonucleotide probe was antisense to the complementary target RNA sequence. Each DNA oligonucleotide probe was also modified with a 5′ biotin in order to enable capture of DNA-RNA hybrids on streptavidin coated magnetic beads (described below). While we had previously used 120-mer probes, we found that 90-mer probes provided comparable stringency and yield in the conditions used. For *Xist*, we used 142 probes that covered the entire mature RNA sequence, with the exception of regions that match to other transcripts or genomic regions as previously described[13,34].

*Total cell lysate preparation.* For the 18S and U1 experiments we used total cellular lysates prepared in the following manner. We lysed batches of 20 million cells by completely resuspending frozen cell pellets in ice cold detergent-based Cell Lysis Buffer (10 mM Tris pH 7.5, 500 mM LiCl, 0.5% dodecyl maltoside (DDM, Sigma), 0.2% sodium dodecyl sulphate (SDS, Ambion), 0.1% sodium deoxycholate (Sigma)). Next, 1 × Protease Inhibitor Cocktail (Set III, EDTA-free, Calbiochem) and 920 U of Murine RNase Inhibitor (New England Biolabs) were added and the sample was incubated for 10 min on ice to allow lysis to proceed. During this incubation period, the cell sample was passed 3–5 times through a 26-gauge needle attached to a 1 ml syringe in order to disrupt the pellet and shear genomic DNA. Each sample was then sonicated using a Branson Digital Sonifier with a microtip set at 5 W power for a total of 30 s in intermittent pulses (0.7 s on, 1.3 s off). During sonication the samples were chilled to prevent overheating of the lysate. The samples were then treated for 10 min at 37 °C with 2.5 mM $MgCl_2$, 0.5 mM $CaCl_2$, and 20 U of TURBO DNase (Ambion) to digest DNA. Samples were returned to ice and the reaction was immediately terminated by the addition of 10 mM EDTA and 5 mM EGTA. Disulphide bonds were reduced by addition of 2.5 mM Tris-(2-carboxyethyl) phosphine (TCEP) and samples were then mixed with twice the lysate volume of 1.5 × LiCl/Urea Buffer (the final1 × buffer contains 10 mM Tris pH 7.5, 5 mM EDTA, 500 mM LiCl, 0.5% DDM, 0.2% SDS, 0.1% deoxycholate, 4 M urea, 2.5 mM TCEP). Lysates were incubated on ice for 10 min then cleared by centrifugation in an Eppendorf 5424R centrifuge for 10 min at 16,000*g*. Supernatants were pooled and flash frozen in liquid nitrogen for storage at −80 °C.

*Nuclear lysate preparation.* For the *Xist* versus U1 and 45S versus U1 comparisons, we used nuclear lysates prepared in the following manner. We lysed batches of 50 million cells by resuspending frozen pellets in 1 ml Lysis Buffer 1 (10 mM HEPES pH 7.2, 20 mM KCl, 1.5 mM $MgCl_2$, 0.5 mM EDTA, 1 mM Tris(2-carboxyethyl)-phosphine (TCEP), 0.5 mM PMSF). Then the samples were centrifuged at 3,300*g* for 10 min to pellet cells. The cell pellets were resuspended in 1 ml Lysis Buffer 1 with 0.1% dodecyl maltoside (DDM) and Dounced 20 times using a glass Dounce homogenizer with the small clearance pestle (Kontes). Nuclei released from the cells after Douncing were pelleted by centrifugation at 3,300*g* then resuspended in 550 μl Lysis Buffer 2 (20 mM Tris pH 7.5, 50 mM KCl, 1.5 mM $MgCl_2$, 2 mM TCEP, 0.5 mM PMSF, 0.4% sodium deoxycholate, 1% DDM, and 0.1% N-lauroylsarcosine (NLS)). Samples were incubated on ice for 10 min, then each sample was sonicated using a Branson Sonifier at 5 W power for a total of 1 min in intermittent pulses (0.7 s on, 3.3 s off) to lyse nuclei and solubilize chromatin. During sonication the samples were chilled to prevent overheating of the nuclear lysate. Samples were then treated with 2.5 mM $MgCl_2$, 0.5 mM $CaCl_2$, and 330 U TURBO DNase (Ambion) for 12 min at 37 °C to further solubilize chromatin. After DNase treatment, lysates were mixed with equal volume of 2 × Hybridization Buffer (the final 1 × Buffer contains 10 mM Tris pH 7.5, 5 mM EDTA, 500 mM LiCl, 0.5% DDM, 0.2% SDS, 0.1% deoxycholate, 4 M urea, 2.5 mM TCEP). Finally, lysates were cleared by centrifugation for 10 min at 16,000g in an Eppendorf 5424R centrifuge and the resulting supernatants were pooled and flash frozen in liquid nitrogen for storage at −80 °C.

*RNA antisense purification of crosslinked complexes.* Lysates from 200 million or 800 million cells were used for each capture. For 200 million cells the following protocol was used, and scaled appropriately for larger cell numbers. For each capture, a sample of heavy or light SILAC labelled frozen lysate was warmed to 37 °C. For each sample, 1.2 ml of Streptavidin Dynabeads MyOne C1 magnetic

beads (Invitrogen) were washed 6 times with equal volume of hybridization buffer (10 mM Tris pH 7.5, 5 mM EDTA, 500 mM LiCl, 0.5% DDM, 0.2% SDS, 0.1% deoxycholate, 4 M urea, 2.5 mM TCEP). Lysate samples were pre-cleared by incubation with the washed Streptavidin C1 magnetic beads at 37 °C for 30 min with intermittent shaking at 1,100 r.p.m. on a Eppendorf Thermomixer C (30 s mixing, 30 s off). Streptavidin beads were then magnetically separated from lysate samples using a Dynamag magnet (Life Technologies). The beads used for pre-clearing lysate were discarded and the lysate sample was transferred to fresh tubes twice to remove all traces of magnetic beads. Biotinylated 90-mer DNA oligonucleotide probes specific for the RNA target of interest (20 µg per sample, in water) were heat-denatured at 85 °C for 3 min and then snap-cooled on ice. Probes and pre-cleared lysate were mixed and incubated at 67 °C using an Eppendorf thermomixer with intermittent shaking (30 s shaking, 30 s off) for 2 h to hybridize probes to the capture target RNA. Hybrids of biotinylated DNA probes and target RNA were then bound to streptavidin beads by incubating each sample with 1.2 ml of washed Streptavidin coated magnetic beads at 67 °C for 30 min on an Eppendorf Thermomixer C with intermittent shaking as above. Beads with captured hybrids were washed 6 times with LiCl/Urea Hybridization Buffer at 67 °C for 5 min to remove non-specifically associated proteins. Between 0.5 and 1% of the total beads were removed and transferred to a fresh tube after the final wash to examine RNA captures by qPCR (see Elution and analysis of RNA samples). The remaining beads were resuspended in Benzonase Elution Buffer (20 mM Tris pH 8.0, 2 mM $MgCl_2$, 0.05% NLS, 0.5 mM TCEP) for subsequent processing of the protein samples.

*Elution of protein samples.* Elution of captured proteins from streptavidin beads was achieved by digesting all nucleic acids (both RNA and DNA, double-stranded and single-stranded) using 125 U of Benzonase nonspecific RNA/DNA nuclease for 2 h at 37 °C (Millipore, #71206-3). Beads were then magnetically separated from the sample using a DynaMag magnet (Life Technologies) and the supernatant containing eluted *Xist*-specific proteins were precipitated overnight at 4 °C with 10% trichloroacetic acid (TCA). TCA treated protein elution samples were pelleted by centrifugation for 30 min at >20,000*g*, then washed with 1 ml cold acetone and recentrifuged. Final protein elution pellets were air dried to remove acetone and stored at −20 °C until processing for mass spectrometry.

*Elution and analysis of RNA samples.* Beads with hybrids were magnetically separated using a 96-well DynaMag (Life Technologies) and the supernatant was discarded. Beads were then resuspended by pipetting in 20 µl NLS RNA Elution Buffer (20 mM Tris pH 8.0, 10 mM EDTA, 2% NLS, 2.5 mM TCEP). To release the target RNA, beads were heated for 2 min at 95 °C in an Eppendorf Thermomixer C. Beads were then magnetically separated using a 96-well DynaMag (Life Technologies) and the supernatants containing eluted target RNA were digested by the addition of 1 mg $ml^{-1}$ Proteinase K for 1 h at 55 °C to remove all proteins. The remaining nucleic acids were then purified by ethanol precipitation onto SILANE beads (Invitrogen) as previously described[13,34]. DNA probes were removed by digestion with TURBO DNase (Ambion). To quantify RNA yield and enrichment, qPCR was performed as previously described[13].

**Mass spectrometry analysis.** *Preparation of proteins for mass spectrometry.* Proteins from RAP-MS captures were resuspended in fresh 8 M urea dissolved in 40 µl of 100 mM Tris-HCl pH 8.5. Disulphide bonds were reduced by incubation with 3 mM TCEP for 20 min at room temperature, followed by alkylation with 11 mM iodoacetamide for 15 min at room temperature in the dark. Samples were then digested with 0.1 µg endoproteinase Lys-C for 4 h at room temperature. After Lys-C digestion the samples were diluted to a final concentration of 2 M urea by the addition of 100 mM Tris-HCl pH 8.5, and $CaCl_2$ was added to a final concentration of 1 mM. Tryptic peptides were generated by treatment with 0.1 to 0.5 µg of trypsin overnight at room temperature. Contaminating detergents were removed from peptides using HiPPR detergent removal columns (Thermo), and peptides were protonated by the addition of 5% formic acid before desalting on a Microm Bioresources C8 peptide MicroTrap column. Peptide fractions were collected and lyophilized, and dried peptides were resuspended in 0.2% formic acid with 5% acetonitrile.

*Mass spectrum measurements.* Liquid chromatography-mass spectrometry and data analyses of the digested samples were carried out as previously described[35] with the following modifications. All experiments were performed on a nanoflow LC system, EASY-nLC 1000 coupled to a hybrid linear ion trap Orbitrap Elite mass spectrometer (Thermo Fisher Scientific, Bremen, Germany) equipped with a nanoelectrospray ion source (Thermo Fisher Scientific). For the EASY-nLC II system, solvent A consisted of 97.8% $H_2O$, 2% acetonitrile, and 0.2% formic acid and solvent B consisted of 19.8% $H_2O$, 80% acetonitrile, and 0.2% formic acid. For the LC-MS/MS experiments, 200 ng of digested peptides were directly loaded at a flow rate of 500 nl $min^{-1}$ onto a 16-cm analytical HPLC column (75 µm ID) packed in-house with ReproSil-Pur $C_{18}$AQ 3 µm resin (120 Å pore size, Dr. Maisch, Ammerbuch, Germany). The column was enclosed in a column heater operating at 30 °C. After 30 min of loading time, the peptides were separated with a 75 min gradient at a flow rate of 350 nl $min^{-1}$. The gradient was as follows: 0–2% Solvent B (5 min), 2–30% B (60 min), and 100% B (10 min). The Elite was operated in data-dependent acquisition mode to automatically alternate between a full scan ($m/z$ = 400–1,600) in the Orbitrap and subsequent rapid 20 collision-induced dissociation (CID) MS/MS scans in the linear ion trap. CID was performed with helium as collision gas at a normalized collision energy of 35% and 10 ms of activation time.

*MS data analysis.* Thermo RAW files were searched with MaxQuant (v 1.5.0.30)[36,37]. Spectra were searched against all UniProt mouse entries (43,565 entries, downloaded 02 Oct 14) and MaxQuant contaminant database (245 entries). Decoy sequences (reversed peptide sequences) were generated in MaxQuant to estimate the false discovery rate[38]. Search parameters included multiplicity of 2 with heavy Arg (+10.0083) and heavy Lys (+8.0142) as heavy peptide modifications. Variable modifications included oxidation of Met (+15.9949) and protein N-terminal acetylation (+42.0106). Carboxyamidomethylation of Cys (+57.0215) was specified as a fixed modification. Protein and peptide false discovery rates were thresholded at 1%. Precursor mass tolerance was 7 p.p.m. (or less for individual peptides). Fragment mass tolerance was 0.5 Da. Requantify and match between runs were both enabled. Trypsin was specified as the digestion enzyme with up to 2 missed cleavages.

**Identification of RNA-interacting proteins.** Proteins of interest from RAP-MS captures were identified based on several criteria. First, proteins were considered identified only if 2 or more unique peptides were found in the mass spectrum. Then proteins of interest were selected based on the SILAC ratio of capture versus control samples. SILAC ratios for each peptide were calculated based on the intensity ratios of heavy and light SILAC pairs. The protein ratio is the median of all calculated peptide ratios, with a minimum of two SILAC pairs required for a SILAC ratio to be assigned to a given protein. A SILAC ratio cutoff of ≥ 3.0 (fold enrichment over control sample) was used as a cutoff for further analysis. We excluded known contaminants, including human keratin and proteins introduced during the sample purification and preparation process (such as streptavidin, benzonase, and trypsin), as well as naturally biotinylated proteins that contaminate the preparation by binding to streptavidin beads.

**RAP-MS experiments and controls.** *18S rRNA versus U1 snRNA.* To validate the RAP-MS method and identify proteins specifically interacting with 18S ribosomal RNA or U1 snRNA, we performed captures of each target RNA in parallel samples from heavy and light labelled lysates from wild-type V6.5 ES cells. The total protein quantity in elution samples from each RAP-MS capture was measured by comparing the median intensity of peptides identified in a single quantitation MS run for each sample. The heavy and light label swapped samples were then mixed equally based on total protein quantity and analysed by mass spectrometry to identify the SILAC enrichment ratio of proteins originating from 18S ribosomal RNA or U1 snRNA captures. The experiment was performed twice and each experimental set contained two biological replicates of 18S and U1 captures (heavy and light labelling states).

*Xist lncRNA versus U1 snRNA captures.* To identify proteins specifically interacting with *Xist* lncRNA, we performed captures as described above with either 200 million or 800 million pSM33 cells treated with doxycycline for 6 h. The total protein quantity in elution samples from each RAP-MS capture was measured by a single quantitation MS run for each sample. Heavy and light label swapped samples were mixed equally based on total protein quantity, and analysed by mass spectrometry. SILAC ratios of *Xist*-enriched proteins versus U1-enriched proteins were calculated and used to identify *Xist*-specific interacting proteins for further analysis. The experiment was performed twice and each experimental set contained two biological replicates of *Xist* and U1 captures, from heavy and light labelled samples. Proteins replicated well between samples, with a sole exception (LBR) that was missed only because its enrichment level (twofold) fell below our enrichment cutoff (threefold) in some replicate samples.

*Xist lncRNA capture from non-crosslinked cells.* As a control to ensure that purified proteins are not non-specifically associated or binding *in vitro* with target RNAs during capture, we performed RAP-MS captures of *Xist* from non-crosslinked cells otherwise treated in the same manner (that is, doxycycline treated for 6 h).

*Xist lncRNA capture from cells where Xist is not expressed.* To confirm that the identified proteins are not resulting from background proteins or probe association with other RNAs or proteins in the pSM33 cells, we performed RAP captures of *Xist* from pSM33 cells that were not treated with doxycycline, but which were otherwise treated identically.

*45S pre-rRNA capture versus U1 capture.* To ensure that the proteins enriched in *Xist* captures using RAP-MS are not simply due to increased protein capture as a consequence of long target RNA transcripts, we additionally performed captures of the 13,000 nucleotide long 45S pre-ribosomal RNA as a control. To ensure specific capture only of the 45S, and not the mature 18S and 28S, we designed

probes that specifically targeted the internal transcribed spacer regions (ITS1 and ITS2) that are only present in the 45S pre-ribosomal RNA. The experiment was performed in the same manner and with the same conditions as the *Xist* lncRNA captures described above. To compare *Xist* protein enrichment to 45S protein enrichment, we used a SILAC approach based on direct comparison of two samples that share a common denominator (called spike-in SILAC[39]). Specifically, we calculated an overall *Xist*/45S SILAC ratio by multiplying the *Xist*/U1 ratio by the U1/45S ratio for each identified protein.

**Protein domain classification.** We defined the conserved domain structures of proteins using the Protein Families database (Pfam[40]).

**RNA immunoprecipitation in UV-crosslinked cells.** We crosslinked pSM33 cells after 6 h of doxycycline-treatment with 0.4 J $cm^{-2}$ of $UV_{254\,nm}$. Cells were lysed and RNA was digested with RNase I to achieve a size range of 100–500 nucleotides in length. Lysate preparations were precleared by mixing with Protein G beads for 1 h at 4 °C. For each sample, target proteins were immunoprecipitated from 20 million cells with 10 μg of antibody (Supplementary Table 1) and 60 μl of Protein G magnetic beads (Invitrogen). The antibodies were pre-coupled to the beads for 1 h at room temperature with mixing before incubating the precleared lysate to the antibody-bead complexes for 2 h at 4 °C. After the immunoprecipitation, the beads were rinsed with a wash buffer of 1 × PBS with detergents. After a dephosphorylation treatment, the RNA in each sample was ligated to a mixture of barcoded adapters in which each adaptor had a unique barcode identifier. After ligation, beads were rinsed with 1 × PBS and detergents and then 5 × PBS (750 mM NaCl) and detergents before pooling 3–4 antibodies in a new tube. The proteins and RNA were then eluted from the Protein G beads with 6 M urea and 40 mM DTT at 60 °C. Protein–RNA complexes were separated away from free RNA by covalently coupling proteins to NHS-magnetic beads (Pierce) and washing 3 times in 6 M GuSCN (Qiagen RLT buffer) and heating in 1% NLS at 98 °C for 10 min. The proteins were then digested with Proteinase K and RNA was purified for subsequent analysis. From the barcoded RNA in each pool, we generated Illumina sequencing libraries as previously described[34]. We saved a small percentage (~1%) of starting material before immunoprecipitation and processed and sequenced this sample in parallel.

**Analysis of crosslinked RNA immunoprecipitation data.** We computed the enrichment for any RNA upon immunoprecipitation with a specific protein relative to its total levels in the cell. To do this, we counted the total number of reads overlapping the RNA in either the immunoprecipitation (IP) sample or the input control. To account for differences in read coverage between samples, each of these numbers was normalized to the total number of reads within the same experiment. This generates a normalized score, per RNA, within each sample. We then computed an enrichment metric by taking the ratio of these normalized values (IP/input). We then compared these enrichment levels across different proteins and controls (that is, IgG). To enable direct comparison across proteins for a given gene, we need to account for differences in the protein specific background level, which may occur to differences in IP efficiency or non-specific binding of each antibody. To do this, we computed a normalized enrichment ratio by dividing the ratio for each gene by the average ratio across all genes for a given protein, as previously described[1].

To exclude the possibility of promiscuous binding to all RNAs, we considered various mRNA controls, which are not expected to bind to these proteins, including *Oct4*, *Nanog*, *Stat3*, and *Suz12*. These mRNAs were selected as examples because they are expressed in ES cells, although many mRNAs show similar results. To account for the possibility that the *Xist* RNA non-specifically binds to any RBP, we evaluated *Xist* with other RBPs that we did not identify as interacting with *Xist* by RAP-MS (PUM1 and HNRNPH). To ensure that a negative result (that is, no enrichment for *Xist*) is meaningful and does not reflect a failed immunoprecipitation experiment, we evaluated Neat1-1, which we previously found immunoprecipitates with hnRNPH[1]. To further evaluate the level of enrichment on other lncRNAs, we considered several lncRNAs including Malat1, Firre, and Tug1. These lncRNAs were selected as examples because they are well-known and expressed in ES cells, although many ES lncRNAs show similar results.

**Immunoprecipitation and RT-qPCR.** Female ES cells were differentiated then crosslinked with UV4k as described above. Pellets of 20 million cells were lysed and treated with TURBO DNase (Ambion) to destroy DNA by incubation for 10 min at 37 °C in an Eppendorf Thermomixer C. The lysate was pre-cleared by incubation with 180 μl of Dynabeads Protein G magnetic beads (Life Technologies). Meanwhile, 10 μg of antibody for immunoprecipitation (SHARP antibody, Novus NBP1-82952 or IgG antibody, Cell Signaling 2729S) was coupled to 60 μl Protein G magnetic beads. After pre-clearing was completed, the lysate was then mixed with the appropriate antibody-coupled Protein G magnetic beads and incubated for 2 h at 4 °C on a Hulamixer sample mixer (Life Technologies) for protein capture. After immunoprecipitation, beads were washed with a wash buffer of 1 × PBS with detergents and then captured nucleic acids were eluted by digesting all proteins with 5.6 U proteinase K (New England Biolabs). Eluted RNA was purified using the RNA Clean and Concentrator-5 Kit (Zima Research) and RT-qPCR was performed as described previously[13] to evaluate RNA enrichment.

**V5-epitope tagged protein expression.** For V5-tagged protein expression and immunoprecipitation, mouse ES cells were electroporated using the Neon transfection system (Invitrogen) with an episomally-replicating vector (pCAG-GW-V5-Hygro) encoding expression of a C-terminal V5 tagged ORF driven by a CAG promoter. ORFs were obtained from the DNASU plasmid repository as Gateway entry clones and inserted into pCAG-GW-V5-Hygro using an LR recombination reaction (Invitrogen). Transfected cells were selected on 125 μg $ml^{-1}$ Hygromycin B (Invitrogen) to generate stably expressing lines.

**siRNA transfections.** For siRNA knockdown experiments, 20 nM siRNAs were transfected using the Neon transfection system (settings: 1,200 V, 40 ms width, 1 pulse). For each transfection, two 10 μl transfections with the same siRNA were carried out in succession using 100,000 cells each, mixed, and plated equally between two poly-L-lysine or poly-D-lysine (Sigma) and 0.2% gelatin (Sigma)-coated no. 1.5 coverslips placed into wells of a 24-well plate containing 2i media. After 48 h, 2i media was replaced and cells on one coverslip of each pair were treated with 2 μg $ml^{-1}$ doxycycline (Sigma) for 16hr to induce *Xist* expression. Coverslips were then fixed in Histochoice (Sigma) for 5 min, washed thoroughly in PBS, and dehydrated in ethanol for storage until FISH staining.

For all proteins we used siRNA pools from Dharmacon (ON-TARGETplus SMARTpool siRNAs). For each of these, we tested whether the siRNA successfully reduced the targeted mRNA expression by >70%. For SAF-A and SMRT, the siRNAs failed to achieve this level of mRNA reduction, so we purchased additional siRNAs (and their associated controls) for SAF-A and SMRT from Qiagen and Ambion respectively, and selected siRNAs that successfully reduced on-target mRNA levels. siRNA against GFP was purchased from Qiagen. For additional independent siRNAs, the siRNAs were purchased as a pool from Dharmacon, Qiagen, and Ambion, or as each individual siRNA deconvoluted from the pool from Dharmacon and Qiagen (Supplementary Table 2).

In addition to the proteins identified by RAP-MS, we knocked down several proteins previously reported to associate with *Xist*, including EED (a component of PRC2)[8], YY1[41], SATB1[42], SRSF1[43], HNRNPC[20], and ATRX[21].

**siRNA experiments in female ES cells.** Female ES F1 2-1 cells were similarly transfected. To initiate differentiation and *Xist* expression for these cells, 2i was replaced with MEF media (DMEM, 10% Gemini Benchmark FBS, 1× L-glutamine, 1× NEAA, 1× penicillin/streptomycin; Life Technologies unless otherwise indicated) at 12 h post-transfection. Forty-eight hours after transfection, 1 μM retinoic acid (Sigma) was administered for 24 h and cells were fixed as described above. For cells not undergoing differentiation, 2i was replaced 12 h and 48 h after transfection.

**Single-molecule RNA FISH.** Single-molecule RNA fluorescence *in situ* hybridization (FISH) experiments were done using QuantiGene ViewRNA ISH Cell Assay (Affymetrix) and QuantiGene ViewRNA ISH Cell 740 Module (Affymetrix) according to manufacturer's protocol. Cells fixed on coverslips were first permeabilized with Detergent Solution QC at room temperature for 5 min, and then incubated with desired mixture of probe set (Affymetrix) in Probe Set Diluent QF at 40 °C for 3 h, followed by incubated with PreAmplifier Mix at 40 °C for 30 min, Amplifier Mix at 40 °C for 30 min, and Label Probe Mix at 40 °C for 30 min sequentially. For DAPI staining, coverslips were incubated in 30 nM DAPI in PBS at room temperature for 15–20 min. Probe set and conjugated fluorophore for FISH were TYPE 1-XIST (550 nm), TYPE 4-GPC4, RBMX, SMC1A, MECP2 (488 nm), TYPE 10-ATRX (740 nm), and TYPE 6-EED1, SHARP, LBR, SAFA, RBM15, MYEF2, PTBP1, HNRNPC, HNRNPM, CELF1, RALY, HDAC3, NCOR2, MID1, PIR (650 nm).

**Immunofluorescence and RNA FISH.** For immunofluorescence (IF), cells were fixed on coverslips and permeabilized with 0.1% Triton-X in PBS at room temperature for 10 min, and blocked with 5% normal goat serum in PBS at room temperature for 10 min. Cells were then incubated with primary antibodies at room temperature for 1 h, followed by incubating with secondary antibodies at room temperature for 1 h. The samples were then processed using the RNA FISH protocol, as described above. Primary antibodies and the dilution used for IF were anti-RNA polymerase II CTD repeat YSPTSPS (phospho S2) (Abcam; ab5095) (1:100), anti-NANOG (Abcam; ab80892) (1:100), and anti-EZH2 (Active Motif; 39933) (1:100). Secondary antibodies and the dilution used for IF were Alexa Fluor 405 goat anti-rabbit IgG (H+L) (Life Technology; 1575534) (1:100) and Alexa Fluor 488 $F(ab')_2$ fragment of goat anti-rabbit IgG (H+L) (Life Technology; 1618692) (1:100).

**Microscopic imaging.** FISH and IF/FISH samples were imaged using a Leica DMI 6000 Deconvolution Microscope with the Leica HC PL APO ×63/1.30 GLYC CORR CS2 objective. Samples stained with TYPE 10-ATRX (740 nm) were

imaged using Nikon Ti Eclipse with the Nikon CFI Plan Apochromat λ DM ×60/1.40 oil objective. Images were projected with maximum projection (3 μm; step size, 0.5 μm).

**X-chromosome silencing assay.** Cells were stained for *Xist* RNA, *Gpc4* mRNA, *Atrx* mRNA and siRNA-targeted mRNA by FISH and imaged. In addition, in some siScramble and siSHARP samples, we used probes against *Rbmx*, *Mecp2*, *Smc1a*, *Mid1* or *Pir* mRNA. Images were then analysed using Matlab R2013b (described below). Cells were selected if the copy number of the targeted mRNA was less than 30% of the level of the no siRNA treated cells and if they induced *Xist* expression. Within these cells, the copy number of *Gpc4* mRNA and *Atrx* mRNA were quantified using a peak finding method (described below) and compared across conditions. We quantified mRNA levels for 50 individual cells. We also evaluated *Xist* expression in siRNA-treated cells, and observed no difference in the percentage of cells that induced *Xist* expression in any of the siRNA conditions relative to untreated cells.

**Quantifying mRNAs by single molecule FISH.** All image analysis was carried out using Matlab (version R2013b) using built-in functions from the Image Processing toolbox. Images were first filtered using a two-dimensional median filter to remove background. Cell boundaries were outlined manually, guided by DAPI staining, to create a binary mask and applied to the various channels from the same field of view. Top-hat morphological filtering, a background subtraction method that enhances the individual focal spots, was applied to the images[44]. The spots were then identified using a 2D peak finding algorithm that identifies local maximal signals within the cell. Once regional maxima were identified, the number of spots was counted for each cell.

**Ezh2 recruitment and Pol II exclusion.** Cells were stained for *Xist* RNA and the siRNA-targeted mRNA (FISH) along with EZH2 or Pol II (IF) as described above. For image acquisition, the exposure time for each individual channel was kept the same across all samples. Images were then analysed and selected for XIST-induced and cells showing knockdown of the target mRNA, as described above. Specifically, the nuclei of individual cells were identified manually using the DAPI staining. We identified the *Xist*-coated territory by using an intensity-based threshold to partition the image within the nucleus and find contiguous 2-dimensional regions of high intensity. The threshold was determined based on the Otsu method as previously described[45], which splits the image into 2 bins—high and low—and identifies a threshold that minimizes the variance within the partition. This creates a binary mask on the image. We visually confirmed that this binary mask accurately reflected the *Xist*-coated territory. We then applied this binary mask to all other images in that field of view (Pol II or EZH2) for all images. We then quantified the intensity of fluorescence signal by taking the average intensity of all the pixels within the region (that is, Pol II or EZH2, respectively). We computed this average intensity (1 number per cell) across all conditions and compared them using a 2-same unpaired *t*-test relative to the scramble sample across 50 single cells.


33. Wutz, A., Rasmussen, T. P. & Jaenisch, R. Chromosomal silencing and localization are mediated by different domains of *Xist* RNA. *Nature Genet.* **30,** 167–174 (2002).
34. Engreitz, J. M. *et al.* RNA-RNA interactions enable specific targeting of noncoding RNAs to nascent pre-mRNAs and chromatin sites. *Cell* **159,** 188–199 (2014).
35. Kalli, A. & Hess, S. Effect of mass spectrometric parameters on peptide and protein identification rates for shotgun proteomic experiments on an LTQ-orbitrap mass analyzer. *Proteomics* **12,** 21–31 (2012).
36. Cox, J. & Mann, M. MaxQuant enables high peptide identification rates, individualized p.p.b.-range mass accuracies and proteome-wide protein quantification. *Nature Biotechnol.* **26,** 1367–1372 (2008).
37. Cox, J. *et al.* Andromeda: a peptide search engine integrated into the MaxQuant environment. *J. Proteome Res.* **10,** 1794–1805 (2011).
38. Elias, J. E. & Gygi, S. P. Target-decoy search strategy for mass spectrometry-based proteomics. *Methods Mol. Biol.* **604,** 55–71 (2010).
39. Geiger, T. *et al.* Use of stable isotope labeling by amino acids in cell culture as a spike-in standard in quantitative proteomics. *Nature Protoc.* **6,** 147–157 (2011).
40. Finn, R. D. *et al.* Pfam: the protein families database. *Nucleic Acids Res.* **42,** D222–D230 (2014).
41. Jeon, Y. & Lee, J. T. YY1 tethers Xist RNA to the inactive X nucleation center. *Cell* **146,** 119–133 (2011).
42. Agrelo, R. *et al. SATB1* defines the developmental context for gene silencing by *Xist* in lymphoma and embryonic cells. *Dev. Cell* **16,** 507–516 (2009).
43. Royce-Tolland, M. E. *et al.* The A-repeat links ASF/SF2-dependent Xist RNA processing with random choice during X inactivation. *Nature Struct. Mol. Biol.* **17,** 948–954 (2010).
44. Theodosiou, Z. *et al.* Automated analysis of FISH and immunohistochemistry images: a review. *Cytometry A* **71,** 439–450 (2007).
45. Fumagalli, M. *et al.* Telomeric DNA damage is irreparable and causes persistent DNA-damage-response activation. *Nature Cell Biol.* **14,** 355–365 (2012).

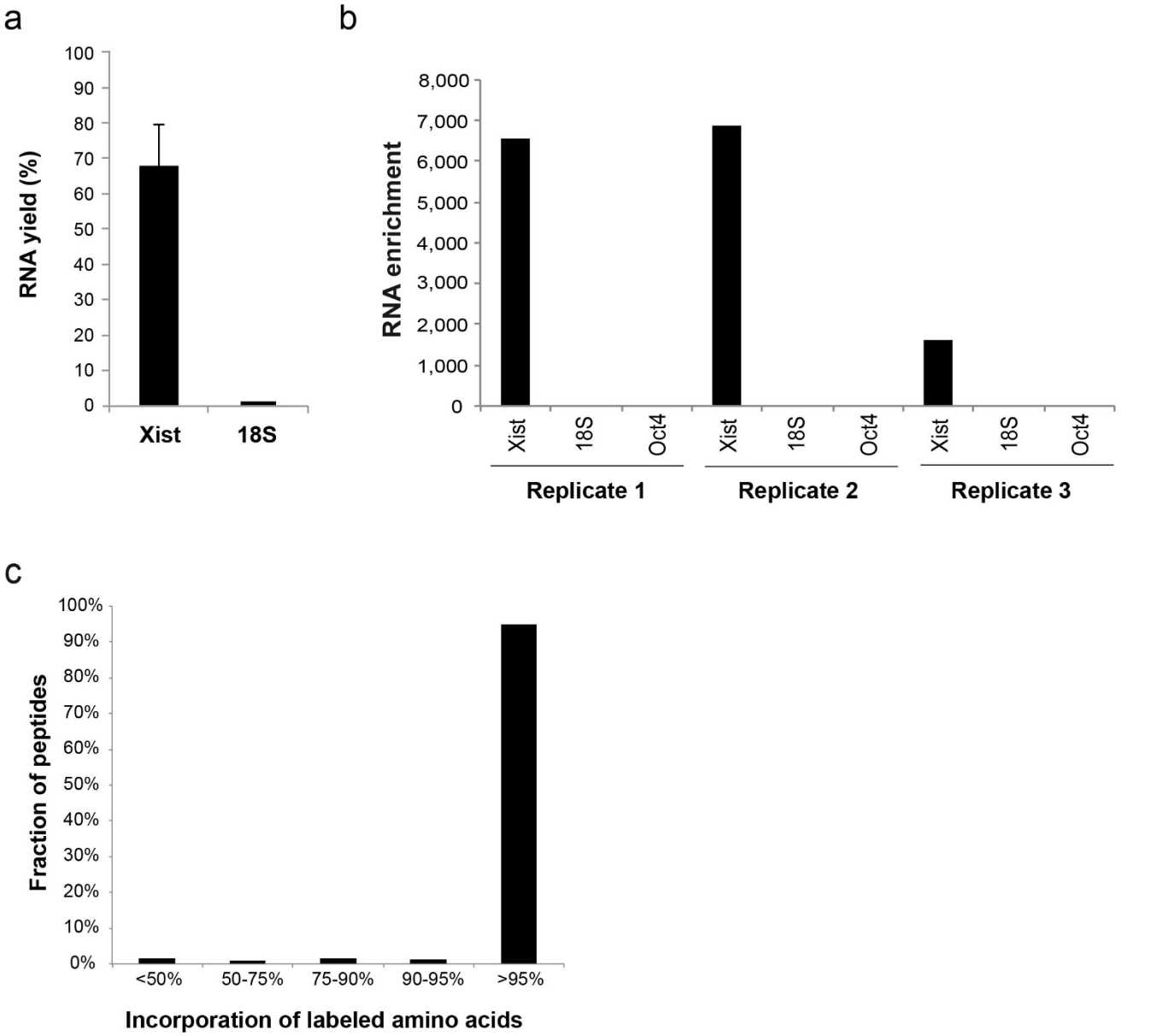


**Extended Data Figure 1 | RAP-MS recovers and enriches the majority of *Xist* RNA from mouse ES cells, and these cells can be efficiently labelled with SILAC.** **a**, RT-qPCR measuring the percentage of the total cellular *Xist* or 18S recovered after RAP-MS of *Xist*. Values are computed as the amount of each RNA in the elution divided by the amount of RNA in the starting ('input') lysate material. Error bars represent the standard error of the mean from 5 biological replicates. **b**, Enrichment of *Xist* after RAP-MS captures from pSM33 cells as measured by qPCR. Bars indicate RNA levels of *Xist*, 18S, and Oct4 after purification of *Xist*, normalized to RNA in input sample. Each bar represents the RNA levels of *Xist*, 18S, and Oct4 after purification of *Xist*, normalized to RNA in input sample, from 3 biological replicates. **c**, SILAC labelling efficiency of a representative culture of pSM33 mouse ES cells after 10 days of growth (3 cell passages) in SILAC medium. Peptides were analysed by mass spectrometry, and values indicate the fraction of identified peptides with heavy-label incorporation with different levels of peptide labelling (shown in bins).

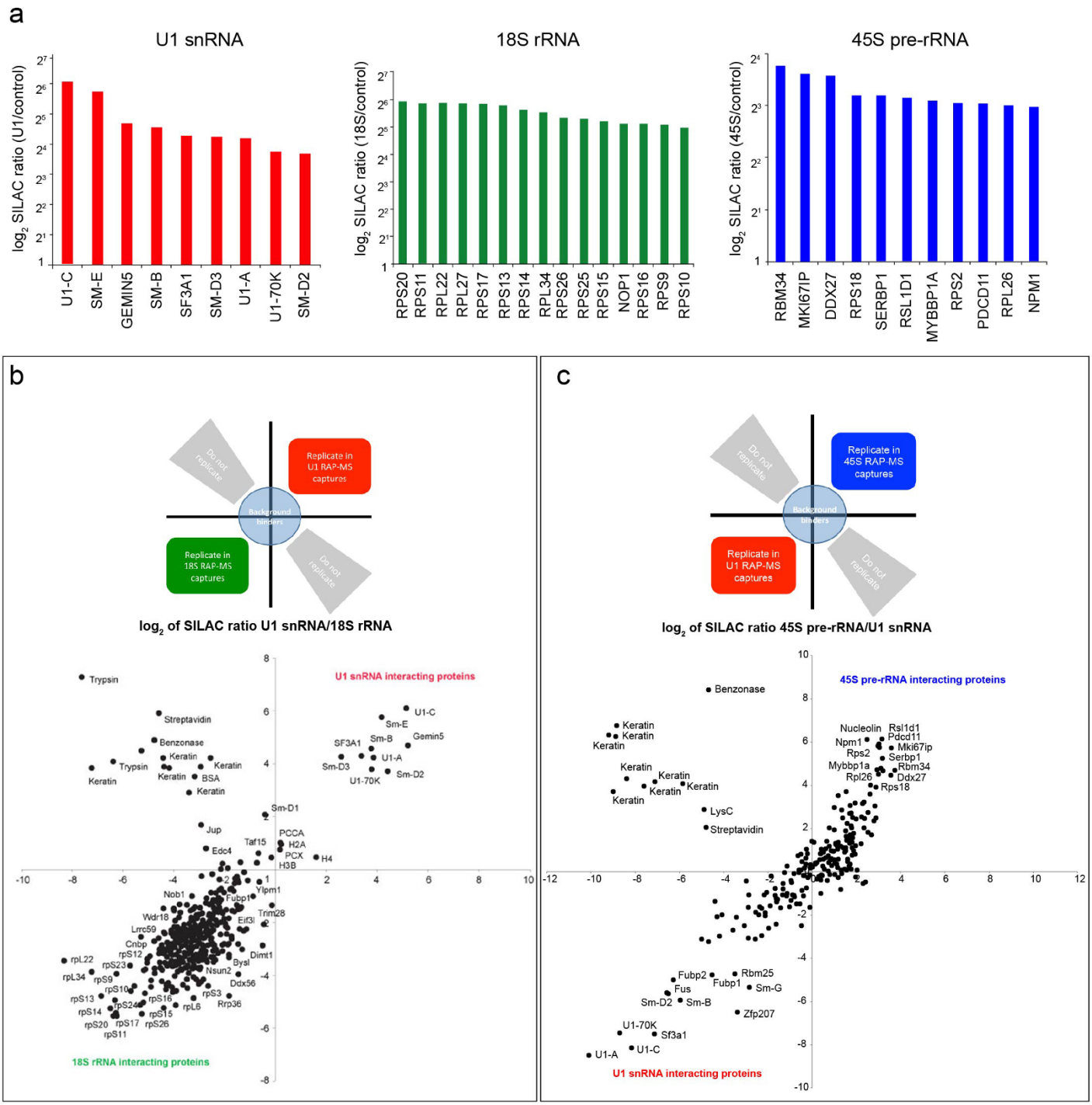


**Extended Data Figure 2 | RAP-MS identifies proteins that are known to directly interact with specific ncRNAs, and separates specific RNA interacting proteins from background proteins.** **a**, SILAC ratios of top proteins enriched in the RAP-MS U1 snRNA, 18S rRNA, and 45S pre-rRNA experiments. **b**, SILAC ratio plot of replicate captures of U1 snRNA versus 18S rRNA from one of two biologically independent label-swap experiments. Proteins associated with U1 are consistently found in U1 samples, both light and heavy labelled (top right quadrant), and proteins specifically associated with 18S are consistently identified in 18S, both light and heavy (lower left quadrant). Background contaminant proteins have low enrichments (centre of panel) or are consistently found in the light channel and do not replicate between experiments (that is, keratin, streptavidin). **c**, SILAC ratio plot of replicate captures of U1 snRNA versus 45S pre-rRNA from one label-swap experiment. Proteins that are known to associate with 45S pre-rRNA are consistently identified in 45S captures.

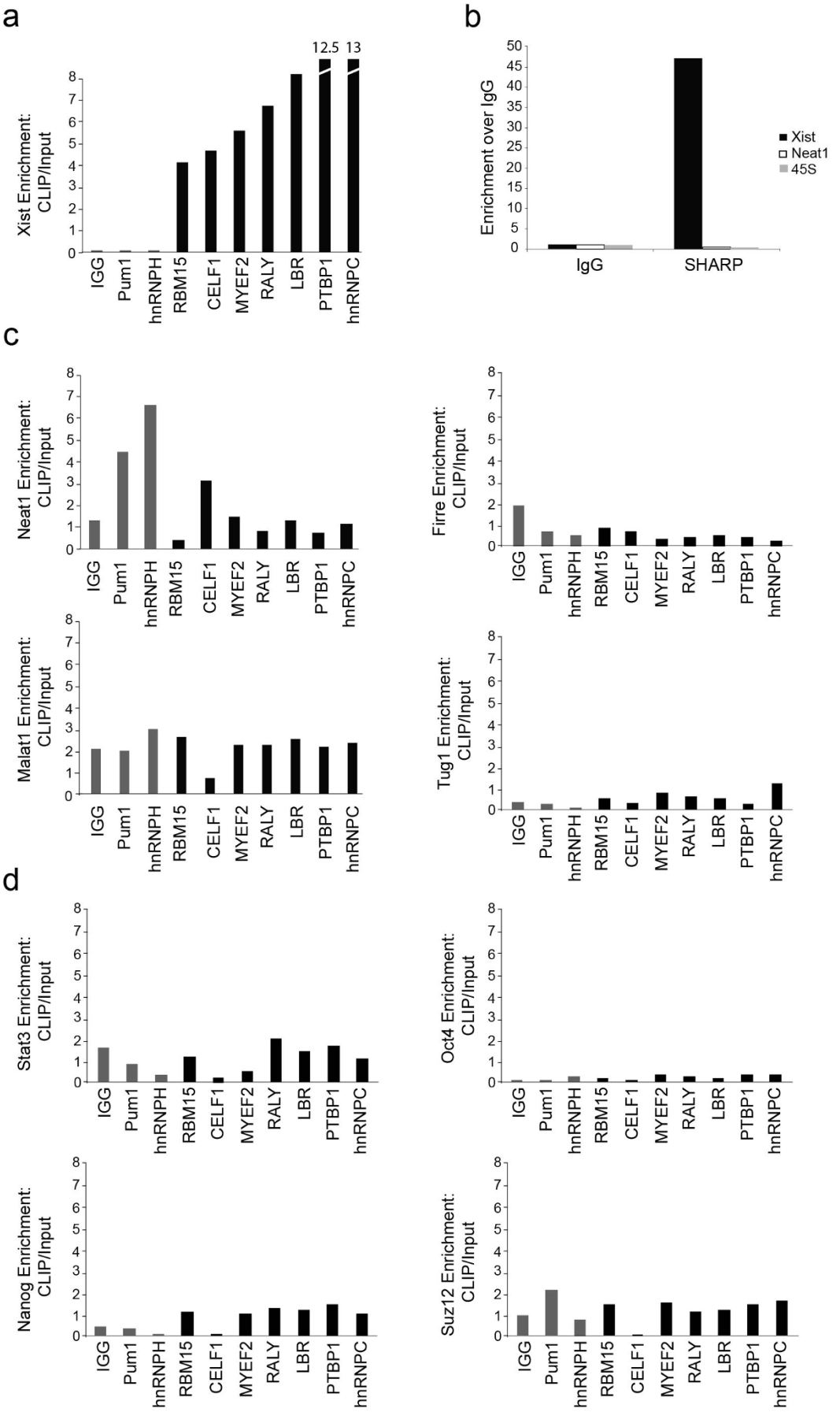

**Extended Data Figure 3 | Immunoprecipitation of the identified *Xist*-interacting proteins confirms *Xist* RNA interaction.** RNA immunoprecipitation experiments were performed for seven *Xist*-interacting proteins (black bars), two control RNA binding proteins that were not identified by RAP-MS and IgG (grey bars) in UV-crosslinked cell lysate after 6 h of *Xist* induction by doxycycline addition (Methods). The RNA associated with each protein was measured and enrichment levels were computed relative to the level of the RNA in total cellular input and normalized to the total efficiency of capture in each sample to allow for direct comparison across all immunoprecipitation experiments (Methods). **a**, Enrichment of the *Xist* lncRNA after immunoprecipitation from a sample of pSM33 male cells. **b**, Immunoprecipitation of SHARP was performed from a sample of UV-crosslinked females ES cells that were treated with retinoic acid for 24 h. The levels of recovered *Xist* lncRNA (black bars), Neat1 lncRNA (white bars), and 45S pre-ribosomal RNA (grey bars) were measured by RT-qPCR. Enrichment of each RNA after capture with anti-SHARP antibody was calculated relative to the level of RNA captured with IgG control antibody. **c**, The enrichment of various lncRNAs after immunoprecipitation in pSM33 male cells—including Neat1, Malat1, Firre, and Tug1—are shown. **d**, The enrichment of various mRNA controls after immunoprecipitation in pSM33 male cells—including Oct4, Nanog, Stat3, and Suz12—are shown.

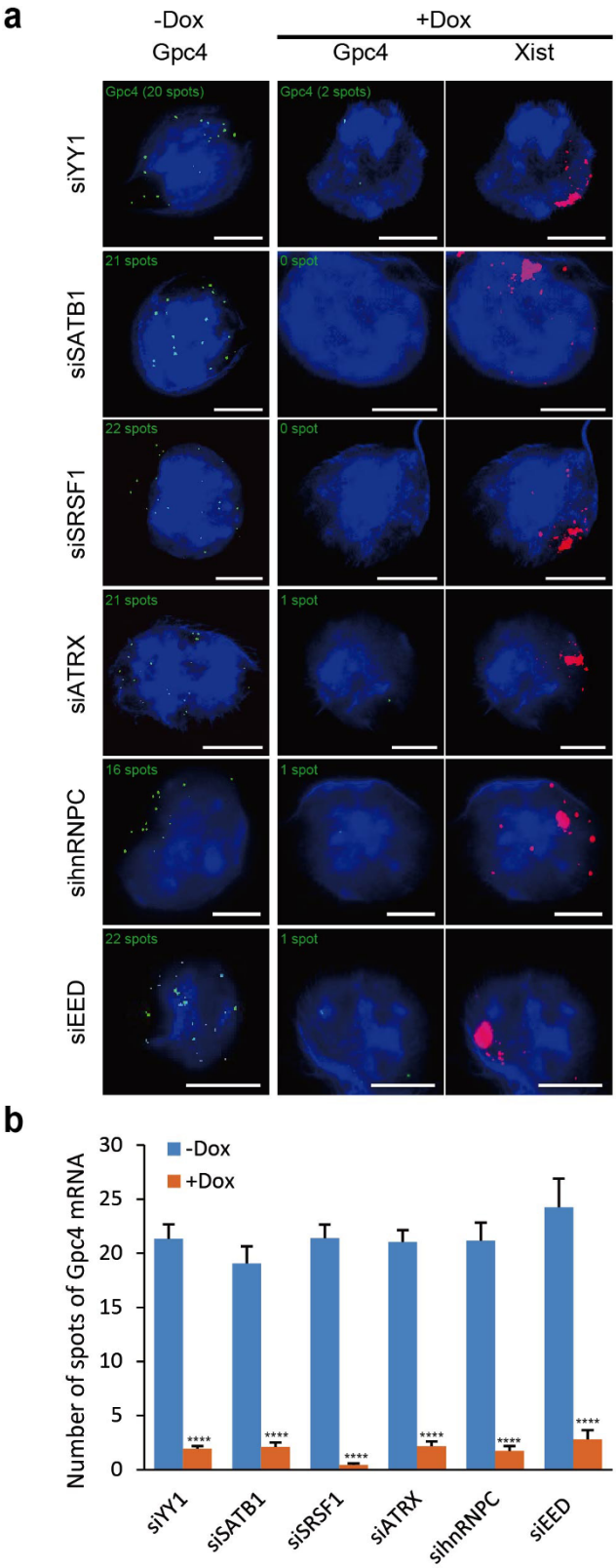


**Extended Data Figure 4 | Previously identified proteins associated with XCI are not required for *Xist*-mediated transcriptional silencing.** **a**, To confirm the specificity of our assay, we tested the function of several proteins that were previously identified to associate with *Xist*, but not to silence transcription, for their role in transcriptional silencing in our inducible male ES cells before *Xist* induction (−Dox; left) or after *Xist* induction for 16 h (+Dox; middle and right). Representative images are shown after knockdown of each protein. DAPI (blue), *Xist* (red), and Gpc4 (green). **b**, Quantification of the copy number of Gpc4 before and after *Xist* induction upon treatment with different siRNAs. Error bars represent the standard error of the mean across 50 individual cells from one experiment. ****$P$ value $< 0.001$ between +Dox and –Dox cells based on an unpaired two-sample $t$-test. Scale bars on the images represent 5 μm. Importantly, while these proteins do not have a role in the initiation of transcriptional silencing, we do not mean to imply that they do not have other roles in XCI.

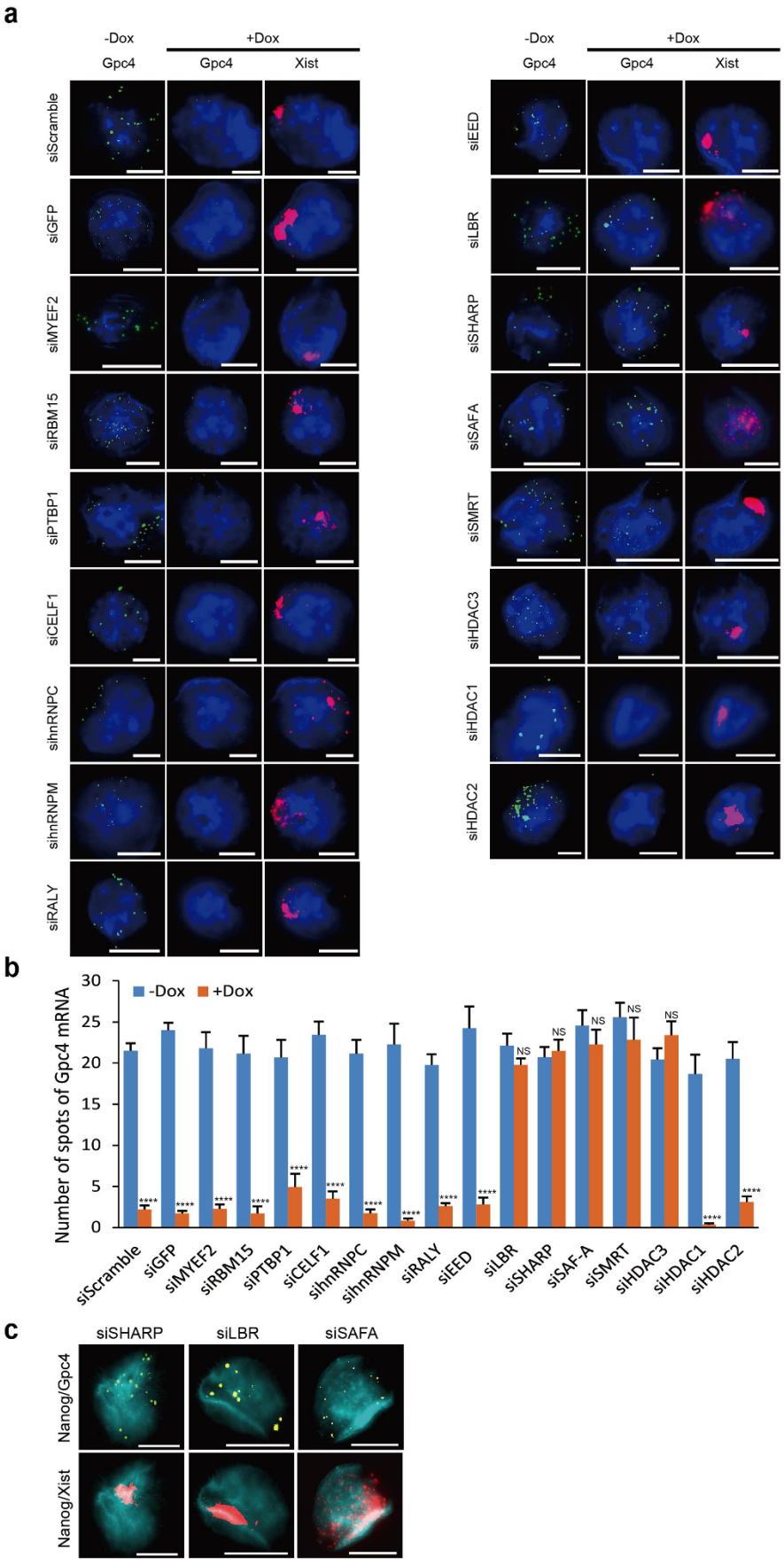

**Extended Data Figure 5 | SHARP, LBR, SAF-A, SMRT, and HDAC3 are required for *Xist*-mediated transcriptional silencing.** **a**, Representative images showing staining of DAPI (blue), *Xist* (red), and Gpc4 (green) for different siRNA knockdown in male ES cells before *Xist* induction (−Dox; left) or after *Xist* induction for 16 h (+Dox; middle and right). **b**, Quantification of the copy number of Gpc4 in –Dox and +Dox cells after knockdown with siRNAs targeting different mRNAs. Error bars represent the standard error of the mean across 50 individual cells from one experiment. NS, not significantly different between +Dox and –Dox cells; ****$P$ value $< 0.001$ between +Dox and –Dox cells based on an unpaired two-sample $t$-test. Scale bars on the images represent 5 μm. **c**, Knockdown of SHARP, LBR, or SAF-A abrogates *Xist*-mediated gene silencing without causing pluripotency defects. Representative images showing staining of Nanog (cyan), *Xist* (red), and Gpc4 (green) upon knockdown of SHARP, LBR or SAF-A after 16 h of *Xist* induction with doxycycline. Scale bars on the images represent 5 μm.

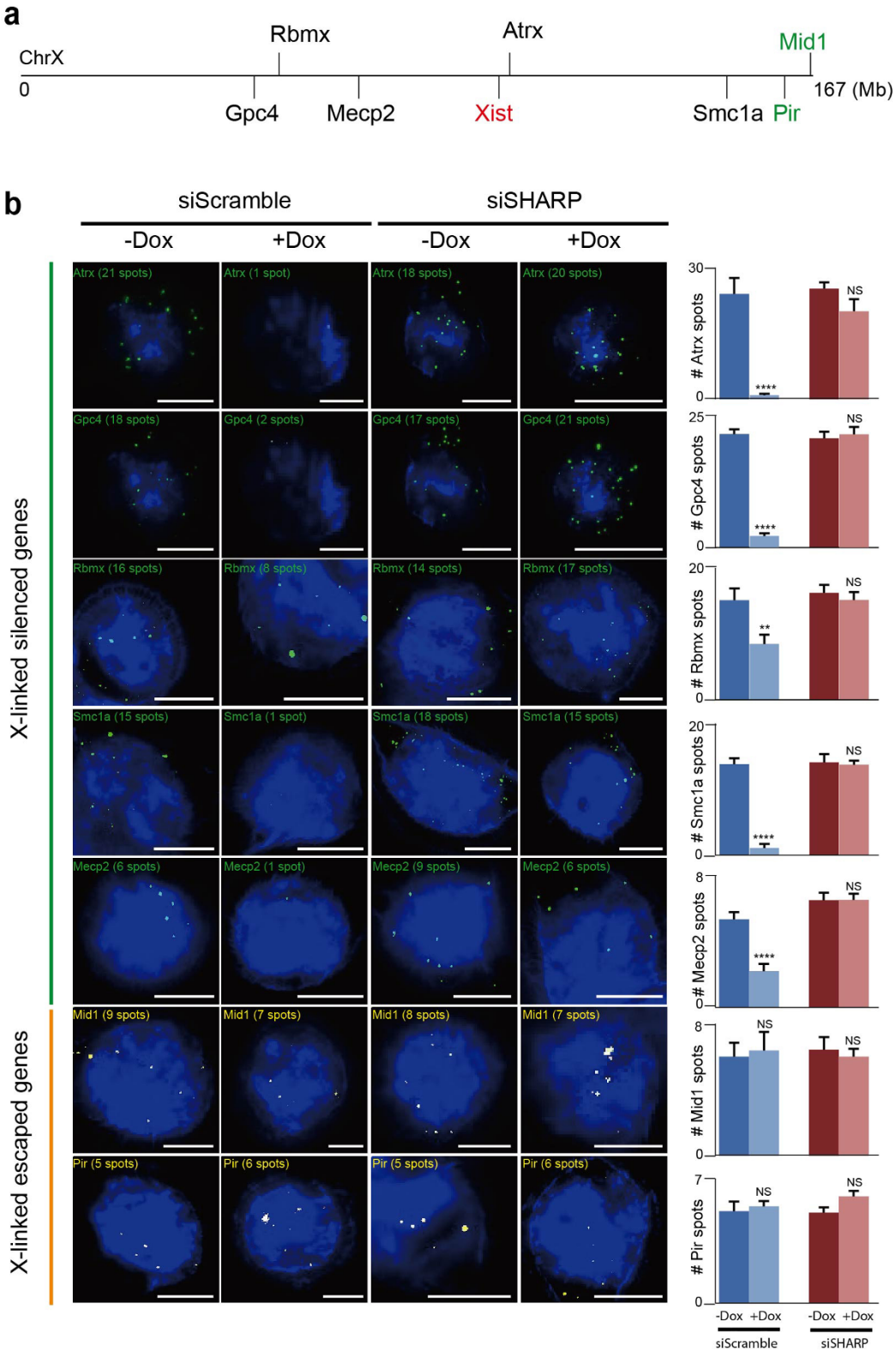


**Extended Data Figure 6 | SHARP is required for silencing many genes across the X chromosome.** **a**, A diagram showing the locations of *Xist* (red), X-linked silenced genes (black), and X-linked escaped genes (green) along the X chromosome. **b**, Representative images showing staining of DAPI (blue), *Xist* (red), X-linked silenced genes (green), and X-linked escaped genes (yellow) upon knockdown of SHARP or control male ES cells before *Xist* induction (−Dox) or after *Xist* induction for 16 h (+Dox). Knock of SHARP abolishes the silencing of Atrx, Gpc4, Rbmx, Smc1a and Mecp2, which are normally silenced upon *Xist* expression, but has no effect on Mid1 and Pir, which normally escape *Xist*-mediated silencing. The bar graphs show the quantification of the copy number of the mRNA for each gene for –Dox and +Dox cells upon transfection with SHARP siRNA or control siRNA; error bars represent the standard error of the mean across 50 individual cells from one experiment. NS, not significantly different, ****$P$ value $< 0.001$, and **$P$ value $< 0.01$ between +Dox and –Dox cells based on an unpaired two-sample $t$-test. Scale bars on the images represent 5 μm.

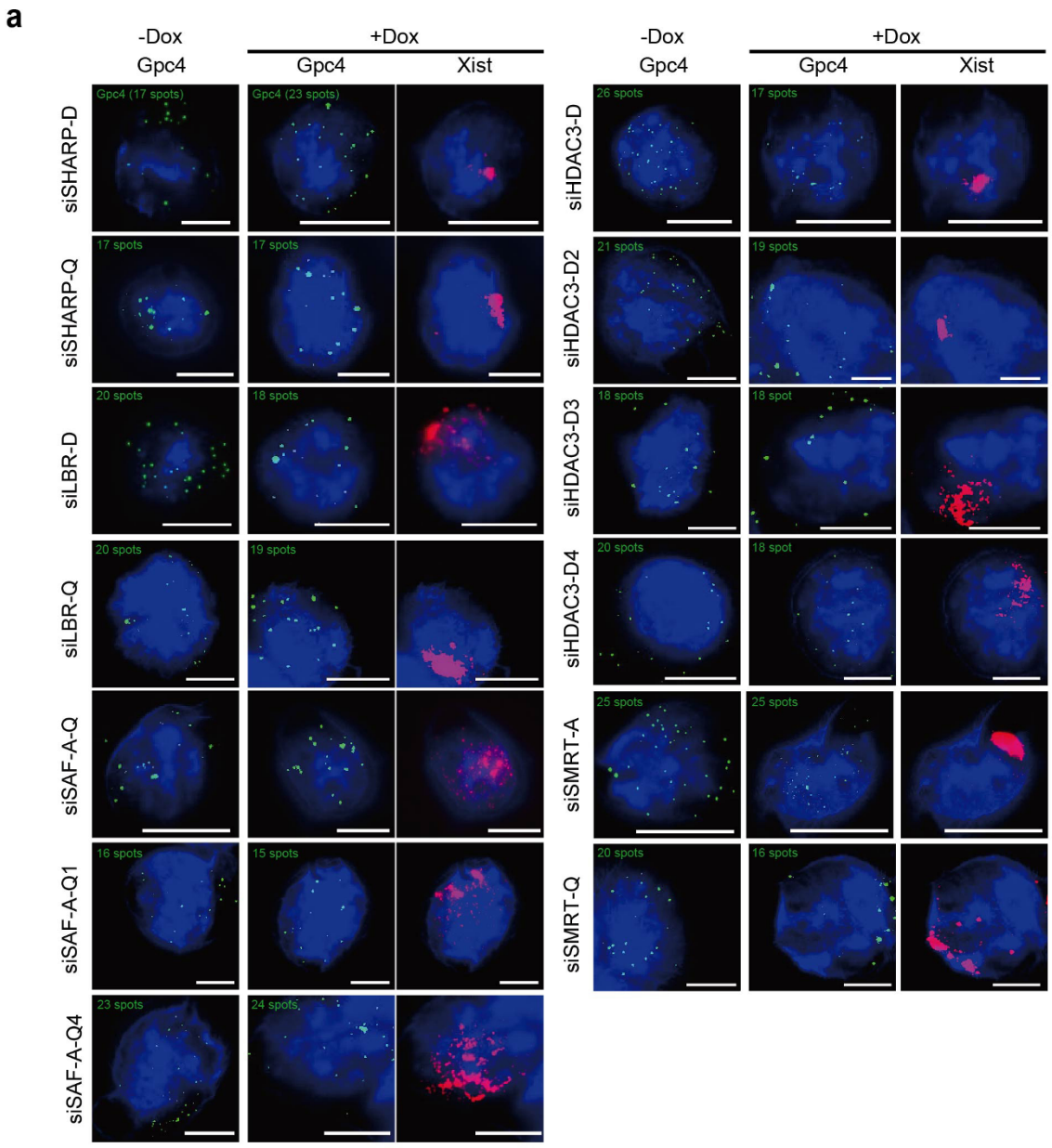

**Extended Data Figure 7 | Multiple independent siRNAs targeting SHARP, LBR, SAF-A, HDAC3, or SMRT demonstrate the same silencing defect.** **a**, Representative images showing staining of DAPI (blue), *Xist* (red), and *Gpc4* (green) after knockdown of proteins using independent, non-overlapping, siRNA pools, or individual siRNA deconvoluted from the pool before *Xist* induction (−Dox; left) or after *Xist* induction for 16 h (+Dox; middle and right). Cells were either transfected with the siRNA pool from Dharmacon (siRNA-D), Qiagen (siRNA-Q) or Ambion/Life Technologies (siRNA-A), or each individual siRNA deconvoluted from the pool from Dharmacon (siRNA-D1, 2, 3, 4) or Qiagen (siRNA-Q1, 2, 3, 4). **b**, Quantification of the copy number of *Gpc4* in –Dox and +Dox cells after knockdown with siRNAs targeting different mRNAs. Error bars represent the standard error of the mean across 50 individual cells from one experiment. NS, not significantly different between +Dox and –Dox cells based on an unpaired two-sample *t*-test. Scale bars on the images represent 5 μm. We excluded all siRNAs that did not reduce the targeted mRNA level by >70% (Methods). The sequences of deconvoluted siRNAs are shown in Supplementary Table 2.

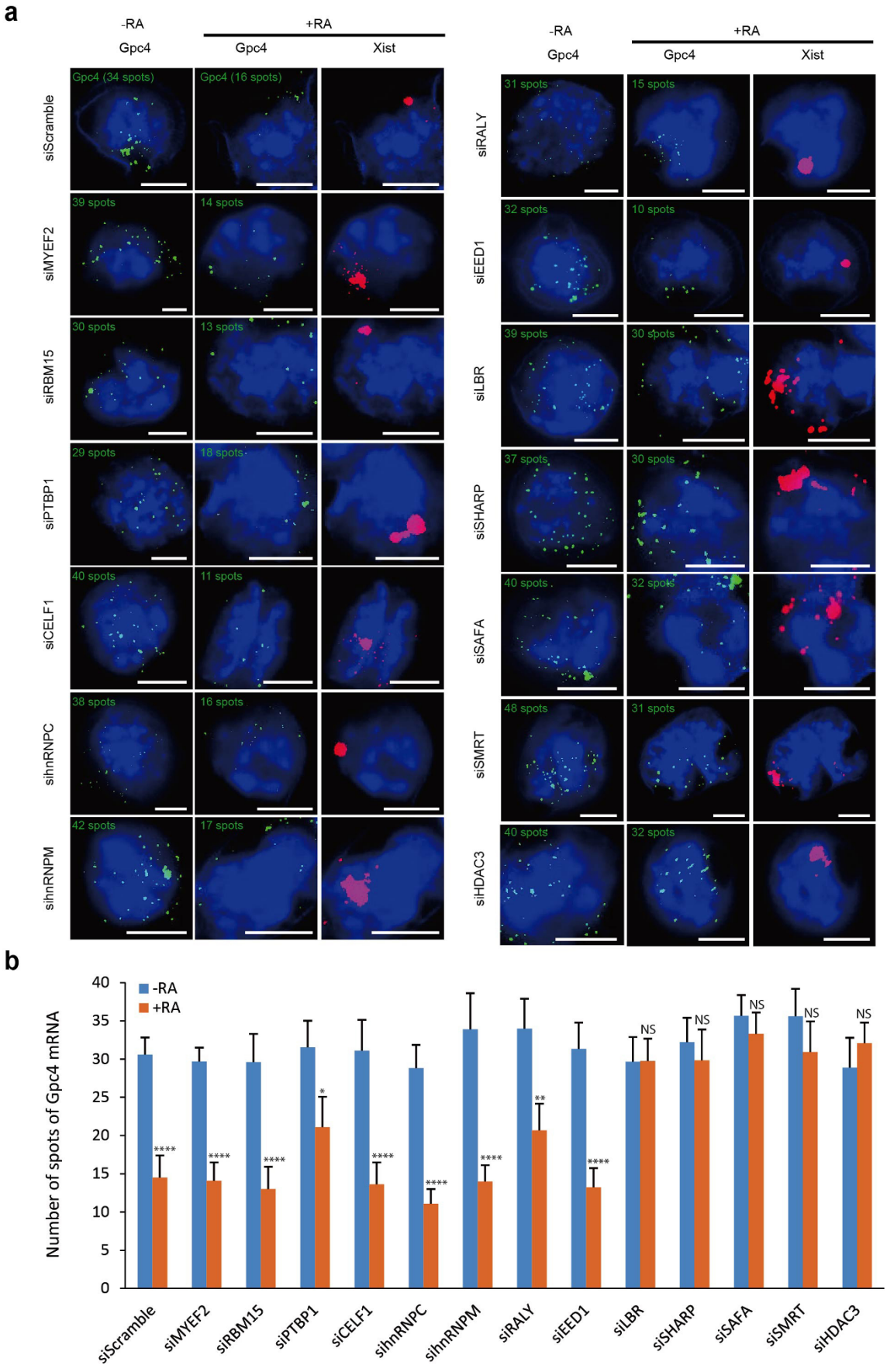

**Extended Data Figure 8 | SHARP, LBR, SAF-A, SMRT, and HDAC3 are required for transcriptional silencing in differentiating female ES cells.** **a**, Representative images showing staining of DAPI (blue), *Xist* (red), and Gpc4 (green) upon knockdown of specific proteins using different siRNAs in female ES cells before differentiation (−RA; left) or after differentiation for 24 h (+RA; middle and right). RA, retinoic acid. **b**, Quantification of the copy number of Gpc4 for –RA and +RA cells upon transfection with different siRNAs. Error bars represent the standard error of the mean across 50 individual cells from one experiment. NS, not significantly different between +RA and –RA cells; ****$P$ value $< 0.001$, **$P$ value $< 0.01$, and *$P$ value $< 0.05$ between +RA and –RA cells based on an unpaired two-sample $t$-test. Scale bars on the images represent 5 μm.

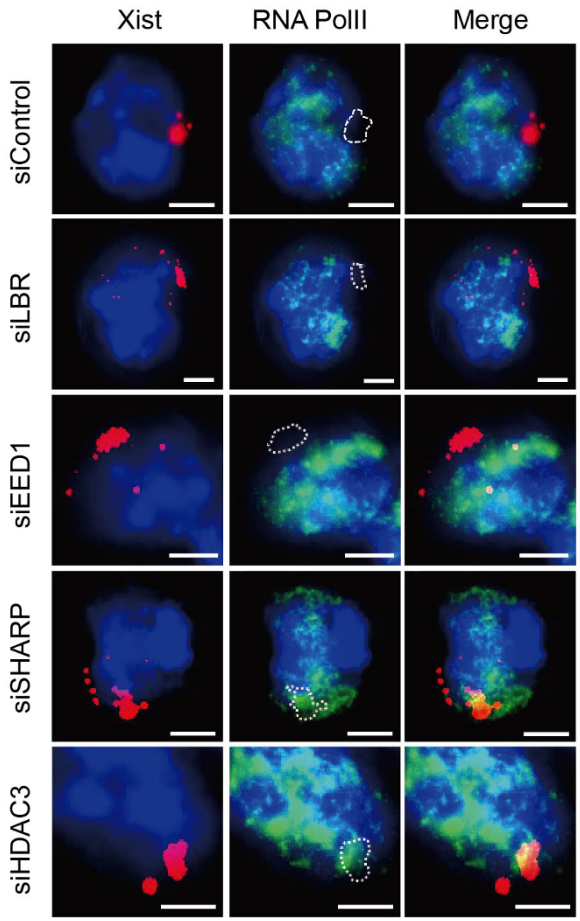


**Extended Data Figure 9 | SHARP is required for exclusion of RNA polymerase II from the *Xist*-coated territory in differentiating female ES cells.** Images of individual cells that are labelled with *Xist* (red), RNA Polymerase II (green), and DAPI (blue) across different siRNA conditions (rows) in female ES cells after 24 h of retinoic acid treatment. The dashed white region represents the outlined *Xist*-coated territory.

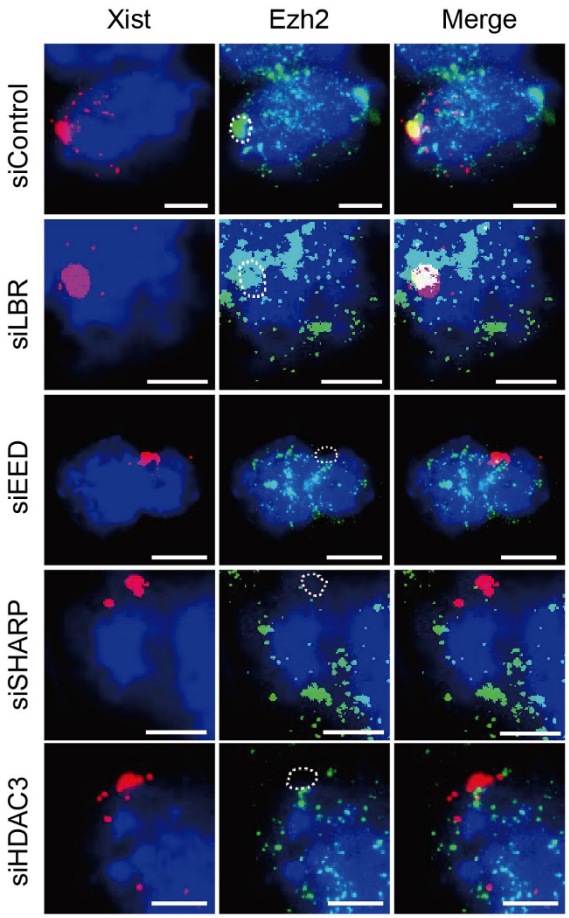


**Extended Data Figure 10 | SHARP is required for PRC2 recruitment across the *Xist*-coated territory in differentiating female ES cells.** Images of individual cells that are labelled with *Xist* (red), Ezh2 (green) and DAPI (blue) across different siRNA conditions (rows) in female ES cells after 24 h of differentiation. The dashed white region represents the outlined *Xist*-coated territory.